CAD/CAE of Blanks for Post-Machining Stretch Forming of Complex Aircraft Panels

Ruibiao Song

A Thesis

In the Department

of

Mechanical and Industrial Engineering

Presented in Partial Fulfillment of the Requirements

For the Degree of Master of Applied Science at

Concordia University

Montreal, Quebec, Canada

April 2014

CONCORDIA UNIVERSITY
School of Graduate Studies

This is to certify that the thesis prepared

By: Ruibiao Song

Entitled: CAD/CAE of Blanks for Post-Machining Stretch Forming of Complex Aircraft Panels

and submitted in partial fulfillment of the requirements for the degree of

Master of Applied Science (Mechanical Engineering)

complies with the regulations of the University and meets the accepted standards with respect to originality and quality.

Signed by the final examining committee:

Dr. A. K. Waizuddin Ahmed   Chair

Dr. Youming Zhang   Examiner

Dr. Liangzhu Wang   Examiner

Dr. Zezhong Chen   Supervisor

Approved by   _____
Chair of Department or Graduate Program Director

_____
Dean of Faculty

Date   _____

ABSTRACT

CAD/CAE of Blanks for Post-Machining Stretch Forming of Complex Aircraft Panels

Ruibiao Song

In this thesis, it mainly focuses on the blank design for the precision stretch forming process of aircraft skin. According to the industry survey and literature review, in the current aerospace industry, the most popular manufacture method for aircraft skin is that the gripper jaws of stretch forming machine hold two ends of the flat blank sheet, stretch and wrap it onto the die to form the desired shape. In this process, the flat blank to be deformed is usually an intact blank sheet with identical thickness. After the deformation, milling process is performed on the curved panel. However, the quality of the curved sheet metal is relatively difficult to be guaranteed since the process of stretch forming would introduce the machining accuracy problem in the milling process.

To improve the quality of the formed part, a new approach is proposed in this thesis for the aircraft skin manufacture. By employing the designed flat blank with pockets pre-machined, the stretch forming process is conducted to form the designed aircraft skin. Comparing with the traditional method that the pockets are machined after the blank deformed, this approach relatively increased the accuracy of pockets positions and shapes and it eliminated the machining difficulty on the curved surface. To study the

feasibility and reliability of this method, the commercial tools of CAD software CATIA and FEA simulation software were utilized for research, in which the CAD data of the FEA simulation output was analysed by the CAD software and then input the modified data to FEA again.

To precisely determine whether the shape and position of the pocket features have met the requirement, the major clue is to evaluate the deformed features in X, Y and Z three directions respectively. Once the formed part is coincidence with the correspondence designed features in these three directions, it means that the designed flat blank could be adopted for stretch forming. To consider the deviation in Z direction, it could be converted to the problem of springback value minimization in Z direction. Due to the large number of factors that influence the springback, optimization method is employed to integrate those possible factors and find the optimal solution. For the deviation in X and Y directions, they are studied through the projection of the profiles on the XY plane. By using shape sensitivity method that judging the influence of two designed blanks offset on the formed pockets profiles, the previous designed flat blank is updated. Comparing the results of different methods, the shape sensitivity method showed a result of efficiently decreasing in the iteration numbers of flat blank design modification and reduction in the shapes deviation between the formed pocket profiles

and the target pocket profiles.

ACKNOWLEDGEMENTS

I hereby wish to express my sincere gratitude and thanks to my supervisor, Dr. Chevy Chen, for his precious guidance and patient tutorials that lead me throughout this work. Not only to mention how extraordinary he is as my supervisor in my research, but also he is truly a teacher of my spirit. It was him who keeps propelling me forward and changes me a lot with the example of his own meticulous attitude on doing researches.

I also need to say special thanks to the people in Bombardier, Jean-Francois Lalonde and Benjamin Larregain. In my research period, they always gave me the valuable instructions in industry standard. Also, their information made my work meaningful with real production.

Additionally, I would like to pass my appreciation to all the dear fellows in our lab, for the tireless help you generously offered when I encountered problems and doubts. I could have needed to face a lot more obstacles to finish this work without your help.

Finally, I give my special thanks to my parents and my fiancee, for giving me all their selfless love, as always, and supporting me in every aspect during my study.

List of Figures

List of Tables

Table of Contents

CHAPTER 1   INTRODUCTION

1.1 Aircraft Skin

In the aircraft design, the skin plays an important role in carrying loads and its quality directly influences the assembling accuracy and lifetime of aircraft. The function of skin is to assemble with stiffeners for transferring the aerodynamic loads acting on the skin onto the frames, so that the shape of the skin is usually designed as the curved sheet panel with several features, like the pockets in the inner side of the skin with certain depth. The properties of features on the skin are varied according to the different assembling purposes. They could have different and irregular shapes, as two samples shown in Figure 1.1. The thickness of the panel is usually around $2mm$ to $3mm$.
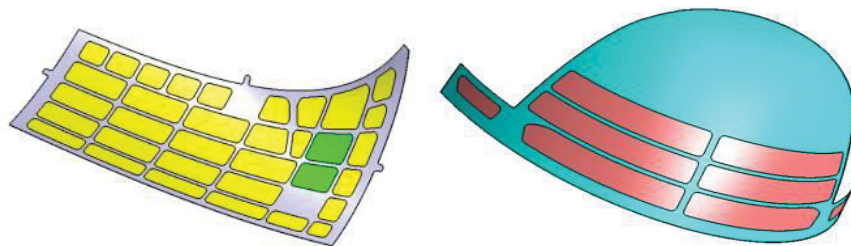
Figure 1.1   Samples of aircraft skins

1.2 Stretch Forming Process

To manufacture the aero structures, it generally enrolls the processes of cold stretching, hot stretch forming, elastoforming, hot forming, superplastic forming and friction welding. Due to the advantages and its ability of large parts manufacture, the stretch forming is worldwide adopted in the aerospace industry, which involves the forming actions, like stretching, bending and twisting that could be achieved by the numerical controlled stretch forming machine, as shown in Figure 1.2.
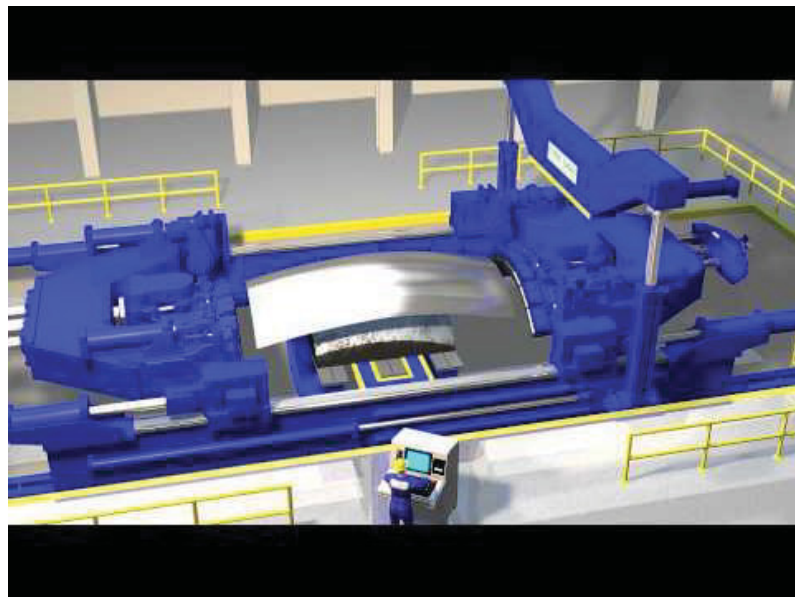
Figure 1.2   Stretch forming machine

In the previous aircraft skin manufacture, the process determination is largely relied on the experience and knowledge of the technicians and the conducted trial

experiments to find the optimal solution. With the development of the numerical controlled technology and its application on the stretch forming machine, more and more researchers have focused on the utilization of numerical simulation with finite element analysis method to study the stretch forming process. By building the model for the forming tools, simulating the kinematic movement of the machine and conducting experiments to obtain the material properties, the sheet panel deformation process is treated as the real manufacture condition, which greatly reduced the experiment time and cost consumption. At the same time, the numerical simulation technology guaranteed and improved the formed part quality.

1.3 Literature Review

A lot of technical articles and relative researches can be found in the field of aircraft skin stretch forming. A. Parris [1] in his Ph.D. thesis focused on the topic of improving of the precision of the stretch forming process. By building a two-dimensional analytical model of the stretch forming operation, it predicted the stresses, strains, springback and also assessed the effects of material parameters variation, pre and post stretch, friction, chemical milling, cross-section and routing. Also, it revealed the significant variation of die table movement, force, strain and separation of the part from

die, a measure of springback. It could say that it introduced most of the related issues

and gave people the general idea about the stretch forming process.

1.3.1 Stretch Forming Process

In the current and most popular stretch forming process method, based on the

designed skin, the stretch machine performs the process onto an intact blank sheet with

uniform thickness. Many researches have been done on the process of stretch forming

to try to improve the quality of the formed part. Wisselink and van den Boogaard [2]

published an article about the delicate relation between material models and forming

limits by modeling the material with the Vegter yield function. The demonstration of the

work hardening and the shape of the yield function both influence the FLC explained the

importance of proper process parameters. The process parameters also could affect the

strain and stress distribution significantly [3, 4, 5, 6]. Zhang and Zhou [3] proposed the

initial loading trajectory of double curve skin through analytic method and combined

finite element analysis and optimization algorithms SQP to acquire the reasonable

loading trajectory. However, the article did not mention how to establish the explicit

function for the optimization objective. In another article published by Zhang and Zhou

[4], it analyzed the possible defects in stretch forming and springback generation

mechanism. Based on the springback value of each independent stretch forming case, they established the respond surface and using NPQLP optimization algorithm under the restrictive of maximal strain to obtain the reasonable process parameters. Han and Wan [5] proposed a method for selecting the major parameters effect on the product quality. The multi-objective problem was dealt as the objective function by transforming the multi-objective problem that concerns sheet metal thinning value and springback value into a single objective function with importance factors and applying the optimization calculation. In this method, it only took two parameters into consideration, which cannot reflect the real manufacture condition though it simplified the calculation. He et al. [6] applied analytical method to determine the loading trajectory and its range by using strain control.

Refer to the stretch forming machine, Liu [7] and He [8] researched on the kinematic movements of stretch forming machine of different models. He and Zhou [7] studied the mechanism of motion according to the FET1200. The motion locus of the clip is calculated by using the theory of gyration tensor and the knowledge of computer graphics. He et al. [8] wrote an article combining the process design, numerical simulation and NC stretch forming. They built the stretch forming equipment VTL1000 NC from Cyril Bath Company and then using geometry analysis method to introduce the

relation between sheet metal deformations and loading of mechanism motion, which integrated the stretch forming process design, analysis and manufacture coincidence with the real manufacture condition.

1.3.2 Optimum Blank Design

In the stretch forming process, besides the importance of the stretch forming process parameters, the proper designed optimal blank is also a key factor that influences the formed part quality. In this thesis, the blank design is an important part of work to obtain the desired aircraft skin. It mainly relates to the location and shape of the features on the flat sheet metal. From the literature review, it could be found that several methods have been developed.

Karima [9], Vogel and Lee [10], Chen and Sowerby [11, 12], Kuwabara and Si [13], Parsa et al. [14] used the slip line field method to obtain the optimum blank. This approach modelled the plastic deformation in plane strain only for a solid part that can be represented as a rigid-plastic body that elasticity is not included and the loading has to be quasi-static. Also it has some limitations, like mentioned in the article of Kuwabara [13] that all this calculation is based on the assumptions that the material is isotropic and the thickness of the blank does not change during the process.

Sowerby et al. [15], Blount and Fisher [16] and Gerdeen and Chen [17] used geometric mapping method to determine the optimum blank. The basic theory of geometric mapping method is trying to find the transformation relationship between designed 3-D part and the blank sheet in 2-D by the point to point mapping. Sowerby et al. [15] described the method of evaluating the strains over the deformed surface by measurements of the nodal points of a grid marked on the undeformed sheet. It could be possible to find the solution for a special case. However, due to the complex behavior of the material and the variation of stretch forming process, any change of the parameters of will result in the transformation modification.

Another optimum blank design method named inverse approach (IA) researched by Barlat [18], Guo et al. [19, 20], Tang [21], Parsa [22]. In the IA method, under the assumption that the deformation follows the minimum work path and the elasto-plastic deformation are independent of the loading path, only two configurations are taken into consideration: the initial flat blank sheet and the 3-D part and. Unlike the geometrical mapping method that only cares about the geometrical relationship, it is also affected by the material properties like yielding criteria, internal force, external force and residual force. Tang et al. [21] proposed an enhanced inverse analysis method by using a robust energy-based 3-D mesh mapping algorithm to obtain the initial solution and then

improve the accuracy. It considered the material and the process parameters to reduce the iteration times. However, for this IA method, the path is only achievable when the principle stretch lines directions fixed with respect to the material during deformation. For the stretch forming with large dimension part, the process could not always follow the proposed path.

Besides the method mentioned above, some other methods are also studied. Toh [23], Kim [24] and Guo [25] used the trial and error method based on the FE method to obtain the optimum blank. Ideal forming was employed by Barlat [26] and Park [27]. Park [27] combined the ideal forming theory with a deformation path iteration method. Shim [28, 29] proposed sensitivity method and Biglari [29] improved the method by ignoring the sensitivity coefficients from the last two iterations, which resulted as a faster solution convergence.

1.4 Limitations of Current Manufacture Method

From the above statement, it has been known that the most popular method for the aircraft skin manufacture is numerical controlled machine performs the stretch forming process and then milling the pocket features on the curved panel. However, the curvature accuracy of the deformed sheet metal after stretch forming is relatively

difficult to be guaranteed and thus it introduces problem in the milling process. First, it is unavoidable to generate springback when the jaws release the part from machine, which causes the curvature error. The curvature error is difficult to be measured so that the milling machine cannot find the accurate machining location. Also, the springback distribution is sensitive to change and hard to be predicted. Second, the location and thickness of the pockets features are not easy to be controlled when milling on the curved surface. The thickness value will be slightly varied at different areas so that the depth to be machined needs further measurement check. And during the milling process, it is always necessary to calculate the curvature at each point since it is no longer the exactly same as the designed curvature because of the springback phenomenon.

1.5 Research Objective

To reduce possibility of machining error and improve the accuracy of pockets position and shape, a new approach is proposed in this thesis by performing the pocket milling process on the flat sheet panel before the stretch forming process. The objective of this thesis is concluded by the following aspects:

Up to now, few researches is found related to the stretch forming of post machined part. In this study, it tried to found the solution of this issue by comparing the

formed features in X, Y and Z three directions with the target profiles. If the accuracy of these three directions reaches the tolerance, the designed blank and stretch forming process could be adopted.

To check the deviation in Z direction, it would be achieved by measuring the springback value in Z direction, which indicates the distance between the formed panel and the die surface. In this way, the kinematic movement of the stretching machine, the stretch forming process and the material properties of the blank to be stretched need to be studied first. Due to the large number of factors considered, optimization method is applied to try to setup the relationship between the stretch forming process parameters and the maximum springback value.

For the deviation in X and Y directions, it could be achieved by using the shape sensitivity method to modify the designed flat blank until it reaches the error requirement.

Combination of the deviation in X, Y and Z three directions, the flat blank with pockets machined could be deformed precisely coincidence with the designed part and the quality of the panel is guaranteed.

1.6 Thesis Outline

In this thesis, it consists of five chapters. CHAPTER 1 gave a general introduction about the aircraft skin, the stretch forming machine and followed by reviewed literatures on this topic. CHAPTER 2 revealed the mechanism of stretch forming machine, stages of the stretch forming process, related material properties and the optimization method to minimize the maximum springback value. CHAPTER 3 focused on the method to reduce the deviation in X and Y directions. A simple case with regular shape is introduced first and then more complex case with multi irregular shapes are solved by sensitivity method. CHAPTER 4 gave two examples with two different types of panels to prove the feasibility and reliability of this blank design method. CHAPTER 5 concluded the blank design method and proposed the possible future work based on this current work.

CHAPTER 2   SPRINGBACK VALUE MINIMIZATION BY THE STRETCH FORMING PROCESS ANALYSIS

2.1 Introduction

As the widespread manufacture process in the aerospace industry, the stretch forming keeps the ability of large parts manufacturing, most often made of Aluminum, with lower tooling costs than the regular drawing tools due to less run. Through the upward movement of the die and the wrapping movement of the jaws that include the deformation of stretching, bending, twisting and their combination, the designed shape of the panel could be formed. According to the current production and research, the major stages employed are wrap forming and additional stretch, or pre-stretch, wrap forming and additional stretch [6]. However, this process is complicated that changing the parameters of process could result in possible defects like over tinning in some area, wrinkle and large springback.

In this chapter, the stretch machine of VTL1000 from Cyril Bath Company will be studied first to find the possible kinematic movement. And then the influence of the parameters of each stage in stretch forming is introduced. The parts of single curvature,

double curvature are included in this chapter.

2.2 Stretching Forming Machine

2.2.1 Introduction to Stretch Forming Machine

In the forming process of aircraft skin, the stretch forming machine could achieve the manufacturing process by stretching the metal beyond its elastic limits and wrapping it around the die to obtain the desired shape, which includes the actions of stretching, bending, compression, twisting and their combinations. The advanced machine enables one step setting up of production runs for certain parts that seem impossible instead of employment of several machines and multiple steps. Its application in the industry has largely improved efficiency in time and cost saving. Since stretch forming machine also keeps the metal under constant tension with the application of one step setting up, it successfully suppressed the possible imperfections such as "cans" or "buckles."

ACB-Aerospace Metal Solutions and Cyril Bath are the two companies that enrolled in the stretch forming machine manufacture. The machines are generally having two categories: transversal stretch presses and longitudinal stretch presses. For the transversal stretch forming machines exert a traction forces in the transversal direction of the metal sheet. The gripper jaws are in line and rigidly mounted. The kinematics

impressed by the machine to the two lines of gripper jaws allows wrapping the part in a direction tangent to the tool throughout the forming process. And for the longitudinal stretch forming machines, it dedicated to the forming of very long sheets and they are equipped with curvable jaws

In this study, the longitudinal stretch forming machine from Cyril Bath Company will be employed for kinematic analysis, stretch forming process simulation and experiment validation. Cyril Bath Company offers the options of transverse/longitudinal VTL series press, T-series (transverse) and L-series (longitudinal) presses. Also the tonnage rating from 150 to 3000 ton is also available. The model selected in this study is VTL1000.

2.2.2 Mechanism Analysis

In this thesis, the numerical controlled machine that used for stretch forming are based on the model of VTL1000 manufactured by Cyril Company as mentioned in the above section. To analyze the kinematic movement and the possible loading trajectory path, it is necessary to have a fully understanding of the machine. In Figure 2.1 , it shows the simplified mechanism of VTL1000 kinematic movement.

The kinematic movement of the machine could be summarized as followed:

1) Translation movement. Carriage motion works for large distance movement along the X direction and tension cylinder is designed for relatively small value of distance along the axis of tension cylinder. These two translation movements realized the function of blank stretching.

2) The revolution of jaws. As Figure 2.2 shows, this movement could be achieved by carriage angulation and jaw oscillation. Same like translation, the carriage angulation is used for large angle and jaw oscillation for fine tuning.

3) Yoke swing. It is designed for adjusting the jaws to keep the end of deforming blank tangent to the surface of die, as Figure 2.3 shows.

4) Jaws curvature. As Figure 2.4 shows, the center jaws could rotate about the axis of the tension cylinder. The inner jaws and outer jaws are adjusted to fitting the jaws along the curvature of designed part.
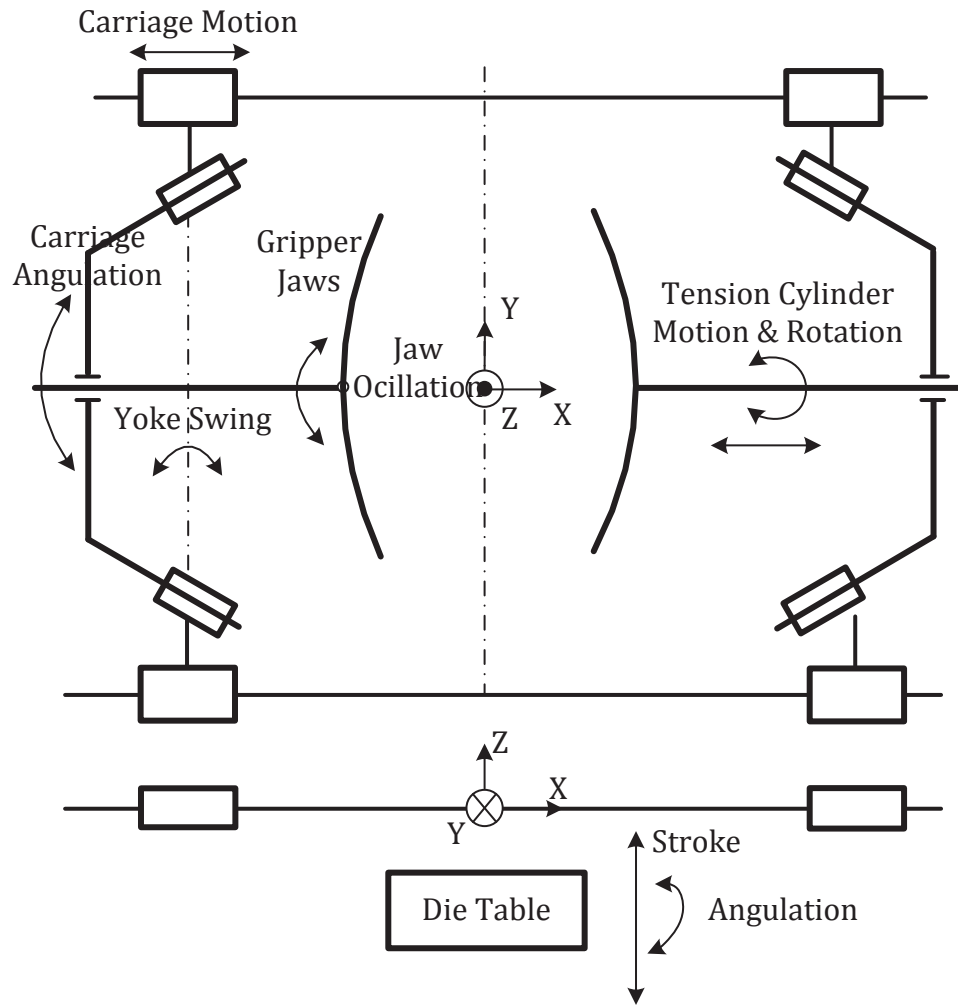
Figure 2.1   Simplified mechanism of VTL1000 kinematic movement
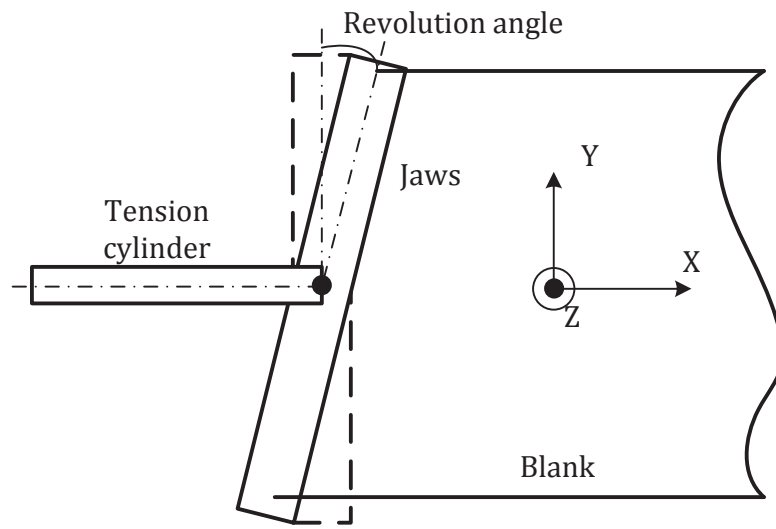
Figure 2.2   Revolution angle of jaws
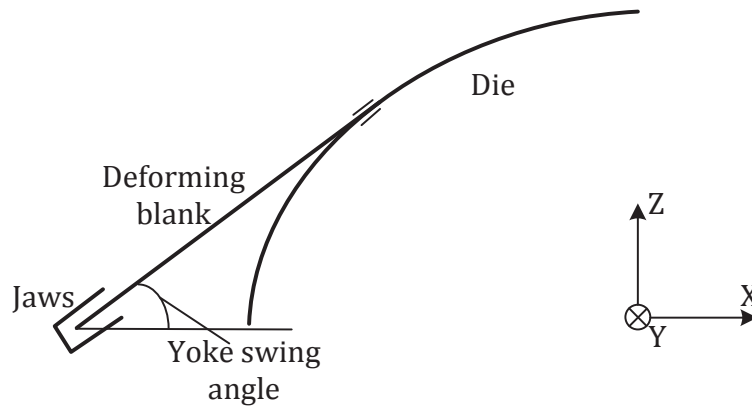
Figure 2.3   Yoke swing angle
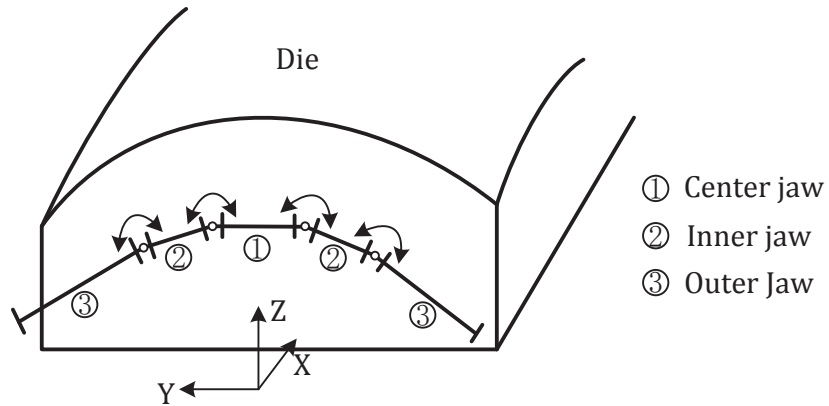
Figure 2.4   Jaws curvature design

2.3 Stages of the Stretch Forming Process

In the stretch forming process, it is generally divided with several stages as pre-stretch, wrap forming, additional stretch, trimming and springback. In this section, each stage will be introduced.

2.3.1 Pre-Stretch Stage

For the pre-stretch stage, the gripper jaws of machine hold the two ends of the blank and move in the outer direction for a certain distance, as Figure 2.5 shows. In the references [30, 31, 32], it has been mentioned that a certain amount of pre-stretch could effectively restrain the springback phenomenon.
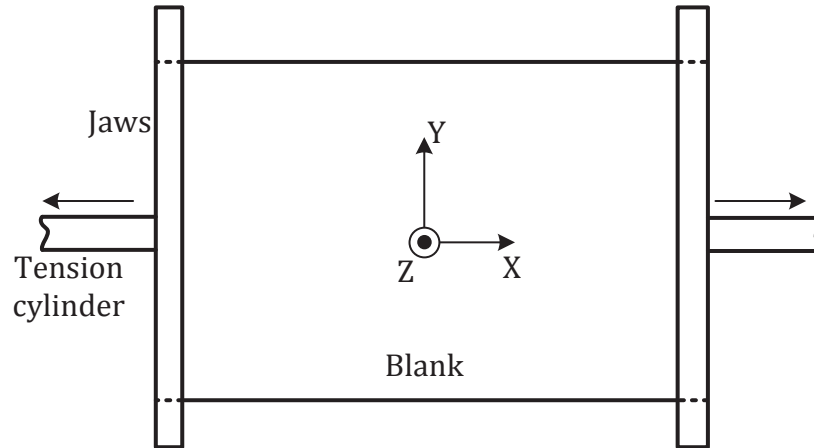
Figure 2.5   Pre-stretch stage

The extension ratio of the blank is defined as

$$e = \frac{l_1 - l_0}{l_0} \times 100\%, \qquad \text{Eq. 2.1}$$

where l_0 represents the length of blank before stretch and l_1 represents the length

after stretch.

2.3.2 Wrap Forming Stage

In this stage, the jaws hold two ends of the blank as the end status of last stage,

the die moves upward and the jaws move toward the center axis at the same time. The

purpose of moving jaws inside is to keep the sheet metal only stay in bending status to

prevent it from having tensile stress. In this procedure, the die moves upward with a

constant velocity and the velocity of the jaws is determined with the condition that the

part of panel not touching the die, which could be regarded as a line in the front view, as

Figure 2.6 shows, always keeps tangent to the spline curve of the die at the end point touching the die.
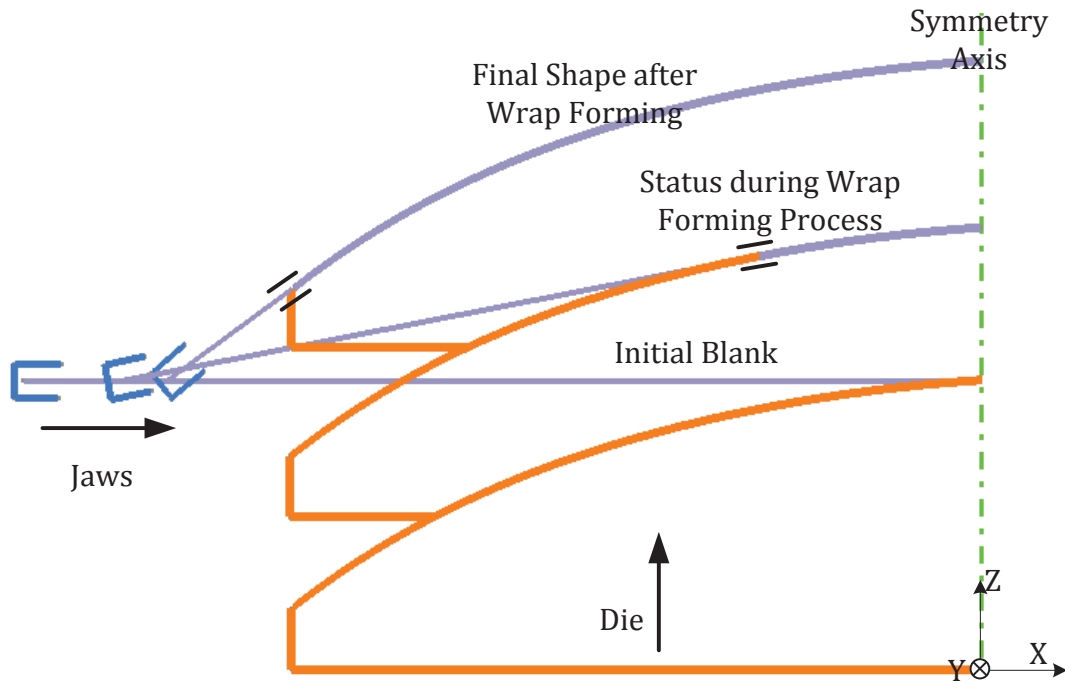
Figure 2.6   Wrap forming stage

To obtain the velocity of the jaws, it could be calculated as followed. First, according to the given shape of the die, find numerous points on the spline curve of the die and then use polynomial function for the curve fitting. For example, n points $(P_1, P_2, P_3 ..... P_n)$ are picked up equal length along the curve and then the polynomial function

$$z = a_3 \cdot x^3 + a_2 \cdot x^2 + a_1 \cdot x + a_0 \qquad \text{Eq. 2.2}$$

is applied for curve fitting. Also, according to the polynomial function obtained, the

angle between tangent line and the horizontal direction could be calculated as:

$$\alpha = \arctan\left(\frac{dz}{dx}\right) = \arctan\left(3a_3 \cdot x^2 + 2a_2 \cdot x + a_1\right). \qquad \text{Eq. 2.3}$$

Based on the constant velocity of the die, the process of the wrap forming could be separated into numerous numbers as small step. In each step, the initial and finishing position of the die are known and thus their respect positions of the jaws could be calculated according to the condition that total length of the panel does not change in this stage, so the velocity of the jaws could be calculated as a constant in this small step.

2.3.3 Additional Stretch Stage

The additional stretch stage is followed by the last stage of wrap forming. In this stage, the blank will generate certain plastic deformation, and by conducting this stretch, it could improve the stress, strain distribution in the cross section area, and reduce the springback value [3, 33]. The jaws hold the two ends of the panel and the die moves a certain distance upward, at the same time, the jaws move with the condition that the ends of blank always keep tangent to the die, as we can see from Figure 2.7. Since the velocity of the die and the angle α are known, the velocity of the jaw could be calculated as

$$V_{jaw} = V_{die}\Big/\tan\alpha. \qquad \text{Eq. 2.4}$$

21
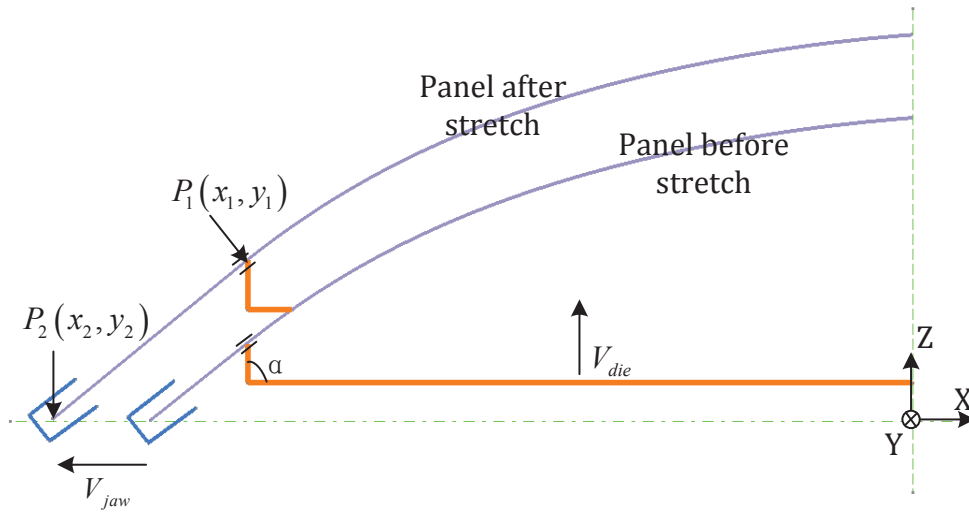
Figure 2.7   Additional stretch stage

The elongation ratio of the panel in this stage could be calculated by using the following equation:

$$e = \frac{\left(\left(x_1 - x_2\right)^2 + \left(y_1 - y_2\right)^2\right)^{1/2} + l_{die} - l_{initial}}{l_{initial}} \times 100\%, \qquad \text{Eq. 2.5}$$

where l_{die} represents the arc length of the die, $l_{initial}$ represents the initial length of the blank.

2.3.4 Trimming and Springback

After finishing the stretch forming process, the redundant material of the panel will be trimmed and then release the formed part from the machine. It usually generates the phenomenon of springback. In the stretch forming process, the bending strain and

tensile strain are the two main kinds of deformations and they are the major reason of

the stress difference between the inner surface and the outer surface, which is also the

fundamental reason of spring back phenomenon [34]. For measuring springback in FEA

simulation, it is usually necessary to remove all rigid body motions to be sure that only

springback phenomenon will be analyzed. This can be done by putting nodes of the

blank in objects and defining Cartesian kinematics attribute on them, like the locking

definition for the half model shown in Figure 2.8. The definitions of the locking are Node

A: lock in translation T_Y and T_Z; Node B: lock in translation T_Z, so the degree of

freedom is locked as followed:

Symmetry plane (YOZ):

➢ T_X degree of freedom is locked

➢ R_Y degree of freedom is locked

➢ R_Z degree of freedom is locked

(Node A-Node B)line is parallel to Y, and these nodes are locked in Z:

➢ T_Z degree of freedom is locked

➢ R_X degree of freedom is locked

Node A is locked in translation Y

➢ T_Y degree of freedom is locked
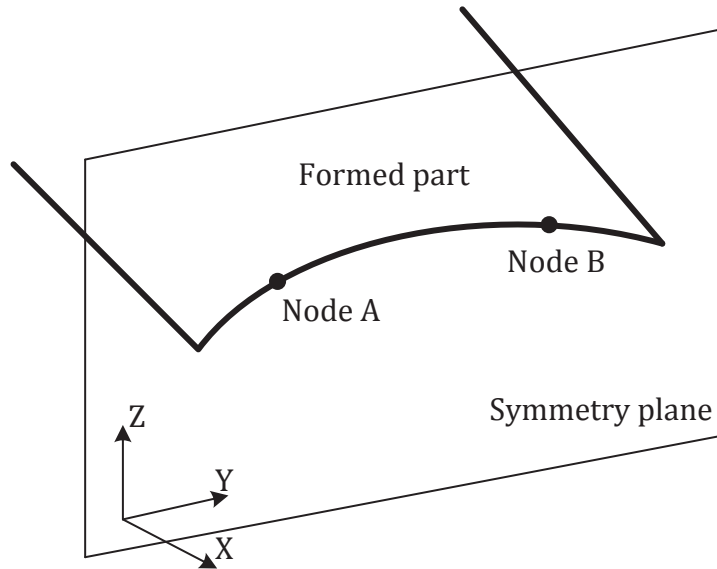
Figure 2.8   Locking definition for half model

2.4 Material Properties

In the stretch forming process, the blank undergoes the complex deformation of elastic and plastic. To simulate these deformation processes, the material properties and its parameters need to be precisely determined. The material selected in this research is Aluminum Alloy 2524T3 and all the studies all based on the properties of this type of material.

2.4.1 Characteristics

The behavior of orthotropic elements is isotropic in elasticity and orthotropic in plasticity. Several plasticity criteria are proposed, such as the HILL 48 criterion, HILL 90

criterion, the BARLAT's criterion, the Corus-Vegter and the Mooney Rivlin law. For aluminum, it is found that HILL 90 criterion is well adapted [35, 36].

Besides the material law, the following data are necessary for material definitions that do not depend on the material law:

1) Thickness;

2) Young's modulus E;

3) Poisson's coefficient ν;

4) Density ρ;

5) Rolling direction.

2.4.2 HILL 90 Material Law

The HILL 90 criterion is based on a non-quadratic yield function. This criterion is able to take into account different behaviors during the bending/unbending phase and seems to be well adapted to aluminum. The HILL 90 criterion models plasticity convex in a more general manner than HILL 48. For HILL 90 material law, the yield function is written as:

$$\left| \sigma_x + \sigma_y \right|^m + \alpha^m \left[\left(\sigma_x - \sigma_y \right)^2 + 4\sigma_{xy}^2 \right]^{\frac{m}{2}}$$

$$+ \left[\sigma_x^2 + \sigma_y^2 + 2\sigma_{xy}^2 \right]^{\frac{m}{2}-1} \cdot \left\{ \beta \left(\sigma_x^2 - \sigma_y^2 \right) + \gamma \cdot \left(\sigma_x - \sigma_y \right)^2 \right\}, \qquad \text{Eq. 2.6}$$

$$= \left(1 + \alpha^m + \beta + \gamma \right) \cdot \left(\sigma_y^1 \right)^m$$

$$= \left(2\sigma_y^b \right)^m$$

where σ_y^1 is the yield stress under uni-axial tension on rolling direction, σ_y^b is the yield stress under equi-biaxial tension. α, β, γ and m are the coefficients of material dependent. They could be calculated based on an iterative method that minimizes a function whose variables are yield stresses and the anisotropy coefficients (least square method).

2.4.3 Forming Limit Diagram

A forming limit diagram (FLD) is a diagram containing measured major/minor strain points on a formed part. A FLD can distinguish between safe and necked, or failed, points. The transition from safe to failed points is defined by the forming-limit curve (FLC) as Figure 2.9 shows.
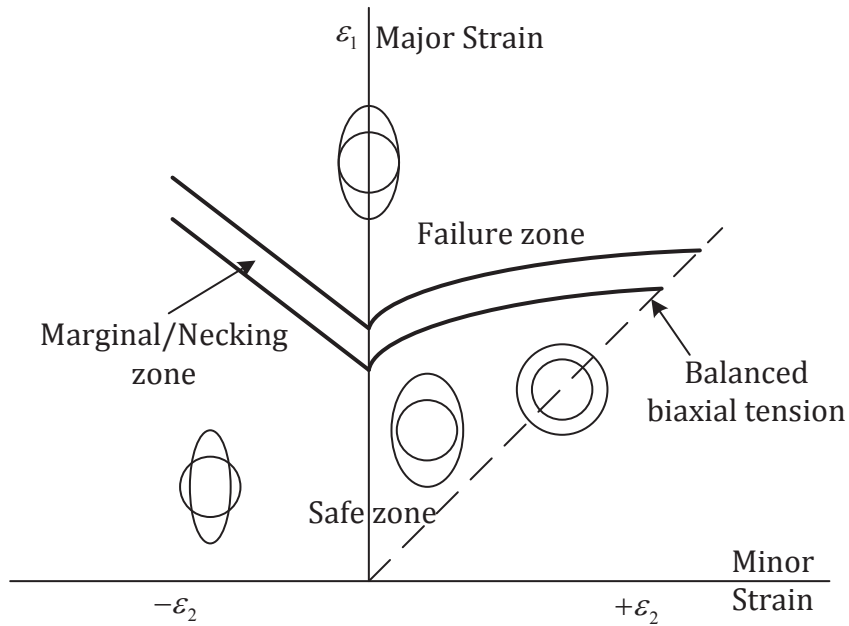
Figure 2.9   Forming limit diagram

To obtain the FLD, a pattern of precise gauge length of appropriate size is applied

to the flat surface of a metal sheet test piece, then the test piece is formed until fracture,

and the percent change in the gauge length in the major direction and in the minor

strain direction at 90°. This is measured to determine the forming-limit under the

imposed strain conditions. Then determine the percent strains ε_1 and ε_2 as followed.

The percent strains can be calculated using

$$\varepsilon_1 = \frac{l_1 - l_0}{l_0} \times 100 \qquad\qquad \text{Eq. 2.7}$$

and

$$\varepsilon_2 = \frac{l_2 - l_0}{l_0} \times 100. \qquad\qquad \text{Eq. 2.8}$$

Plot ε_1 against ε_2 on a forming limit diagram. The major strain ε_1 is plotted along the Y axis and the minor strain ε_2 is plotted along the X axis. And draw the forming-limit curve through the points of maximum ε_1 strain.

2.5 Determination of Stretch Forming Loading Trajectory

In the stretch forming process of aircraft skin, the loading trajectory of the jaws is a key factor for high quality of the product. In this section, the equivalent finite element model used for simulation is established in commercial FEA software. The kinematic movement of the machine and the blank material are all set up based on the previous sections. A calculating method is proposed to obtain the loading trajectory of the machine by combination of the finite element method and optimization algorithms with the objective of achieving the minimum distance between the designed part and the formed part in Z direction, which is known as the springback value.

To illustrate the methodology in this section, an example is employed in this section. For the more complex shape of the die, the jaws could be adjusted as mentioned in the previous section 2.2.2 of the jaws curvature.

2.5.1 Definition of Design Variables

According to previous statement, this stretch forming process includes four stages: pre-stretch, wrap forming, additional stretch and springback. For each stage, certain parameters need to be determined.

In the pre-stretch stage, the jaws hold two sides of the blank to stretch in the horizontal direction, as Figure 2.10 shows. The variables to be determined in this stage is the distance of the jaws movement in each side is $x_1(mm)$ and the velocity of the jaws movement $v_1(mm/s)$. The length of blank reaches to $l_1(mm)$, as

$$l_1 = l_0 + 2 \cdot x_1 .$$ Eq. 2.9
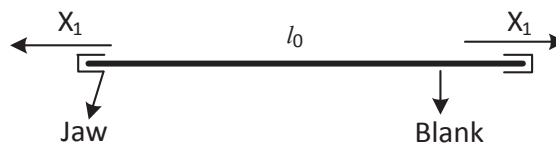
Figure 2.10   Design variable in pre-stretch stage

In the wrap forming stage, the blank is fully wrapped onto the die without stretching, so the movement of the jaws is adjusted according to the position of die and the angle of the jaws always keeps tangent to the curvature of the die at the end touching point of blank and die. The only parameter to be known is the velocity of the die $v_2(mm/s)$ moves upward.

For additional stretch stage, the jaws keep the direction at the end of wrap forming stage and stretch for an additional distance as Figure 2.11 shows. This distance should be considered within the limit without rupture appearance. The parameters in this stage would be the distance of the jaws move $x_3(mm)$ and their velocity $v_3(mm/s)$. The length of the blank at the final state is $l_2(mm)$, as

$$l_2 = l_1 + 2 \cdot x_2$$
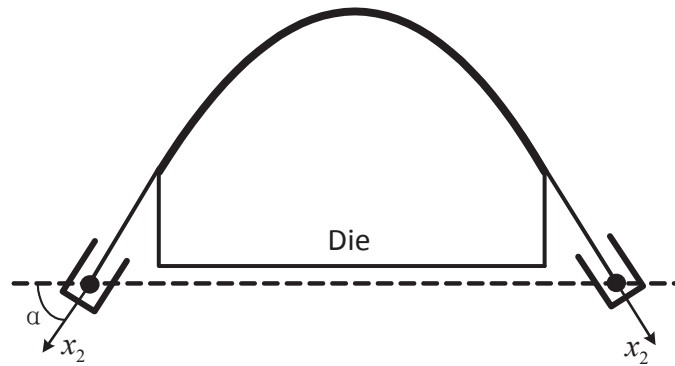
Figure 2.11   Design variable in additional stretch stage

From the above talking, the design variables are summarized in Table 2.1.

Table 2.1   Design variables

Design Variable	x_1	v_1	v_2	x_2	v_3
Unit	mm	mm/s	mm/s	mm	mm/s

2.5.2 Identification of the Criterion to be Optimized

As springback is the most important shape error to consider for the precise of the formed part, it is necessary to minimize the maximum springback value, so the objective

function can be developed as:

$$f = \min\left(\max(u_i)\right) \ i = 1, 2, \cdots, n,$$

Eq. 2.10

where $\max(u_i)$ stands for the maximum springback value in Z direction.

2.5.3 Identification of the Constraints

According to the simulation of the purely stretch in horizontal direction, when one side of jaws reached 62*mm*, the FLD showed that some points dropped in the unsafe zone. If more deformation enrolled, like bending or twisting, the extension length should be less than $62mm$ before the defects begin to appear. Also, to get desired deformation, minimum extension ratio is required as 2%. Thus, the constraint of extension length is set as

$$\frac{1}{2}l_0 \cdot 2\% \leq x_1 + x_2 \leq 62.$$

Eq. 2.11

In this case of study, l_0 is 1720*mm*. For the velocity of the jaws movement, according to the industry survey, it is usually between $1.25mm/s$ and $8mm/s$. So the constraints can be described as:

$$17.2 \leq x_1 + x_2 \leq 62,$$

Eq. 2.12

$$1.25 \leq v_1 \leq 8,$$

Eq. 2.13

$$1.25 \leq v_2 \leq 8,$$

Eq. 2.14

$$1.25 \leq v_3 \leq 8.$$

Eq. 2.15

2.5.4 General Global Search with Meta-Model Numerical Simulation

The objective function is used to evaluate the relationship between the springback value and the parameters of the forming process. According to the above statement, there are five parameters to determine. However, some of these parameters have a significant influence on the final result, and others may have little influence on it. And also due to the large range of these parameters and their internal complex relationship, it is necessary to evaluate their significances to the springback value. First, a research is conducted to roughly learn their relationship by a global search. Usually one cycle of simulation takes 10 to 20 hours depends on the parameters. To find out the explicit objective function, several numerical simulations will be conducted to generate meta-model.

To setup the meta-model, design variables are selected in several levels. Opposite to the full factorial analysis, the Taguchi method reduces the number of experimental runs to a reasonable one, in terms of cost and time, by using orthogonal arrays[37]. Choosing the proper orthogonal arrays suitable for the problem of interest is very important in the Taguchi's approach. Using the method of Sorana D. Bolboaca[38], sixteen levels for five factors are used to conduct the numerical simulations. Table 2.2 is a five-factor sixteen-level orthogonal array of the experimental design and includes the

value of design variables and their corresponding levels.

Table 2.2   Experimental design of five-fator sixteen-level orthogonal array

Exp. No.	Level (Value)				
	$x_1\,(mm)$	$v_1\,(mm/s)$	$v_2\,(mm/s)$	$x_2\,(mm)$	$v_3\,(mm/s)$
1	0(0)	0(1.25)	0(1.25)	0(18)	0(1.25)
2	1(2)	1(1.70)	13(7.10)	9(36)	14(7.55)
3	2(4)	2(2.15)	12(6.65)	13(44)	8(4.85)
4	3(6)	15(8.00)	1(1.70)	1(20)	15(8.00)
5	4(8)	14(7.55)	2(2.15)	15(48)	3(2.60)
6	5(10)	13(7.10)	15(8.00)	2(22)	1(1.70)
7	6(12)	12(6.65)	14(7.55)	8(34)	7(4.40)
8	7(14)	11(6.20)	3(2.60)	14(46)	10(5.75)
9	8(16)	10(5.75)	11(6.20)	11(40)	2(2.15)
10	9(18)	3(2.60)	4(3.05)	12(42)	12(6.65)
11	10(20)	9(5.30)	9(5.30)	4(26)	11(6.20)
12	11(22)	8(4.85)	10(5.75)	3(24)	13(7.10)
13	12(24)	7(4.40)	7(4.40)	7(32)	9(5.30)
14	13(26)	4(3.05)	8(4.85)	6(30)	5(3.50)
15	14(28)	6(3.95)	5(3.50)	10(38)	4(3.05)
16	15(30)	5(3.50)	6(3.95)	5(28)	6(3.95)

Table 2.3 showed the process parameters and the results of simulations.

Table 2.3   Simulation results for each experimental run

Exp. No.	x_1 (mm)	v_1 (mm/s)	v_2 (mm/s)	x_2 (mm)	v_3 (mm/s)	Max. Springback value
1	0	1.25	1.25	18	1.25	19.24
2	2	1.70	7.10	36	7.55	8.63
3	4	2.15	6.65	44	4.85	15.96
4	6	8.00	1.70	20	8.00	12.87
5	8	7.55	2.15	48	2.60	13.2
6	10	7.10	8.00	22	1.70	28.21
7	12	6.65	7.55	34	4.40	15.03
8	14	6.20	2.60	46	5.75	18.60
9	16	5.75	6.20	40	2.15	15.35
10	18	2.60	3.05	42	6.65	9.83
11	20	5.30	5.30	26	6.20	21.5
12	22	4.85	5.75	24	7.10	9.22

13	24	4.40	4.40	32	5.30	13.03
14	26	3.05	4.85	30	3.50	16.78
15	28	3.95	3.50	38	3.05	21.81
16	30	3.50	3.95	28	3.95	14.55

Additionally, the quality of the formed part needs to be checked by FLD. For example, in experimental run No. 8, FLD evaluation figure showed that all the points are in the safe region.
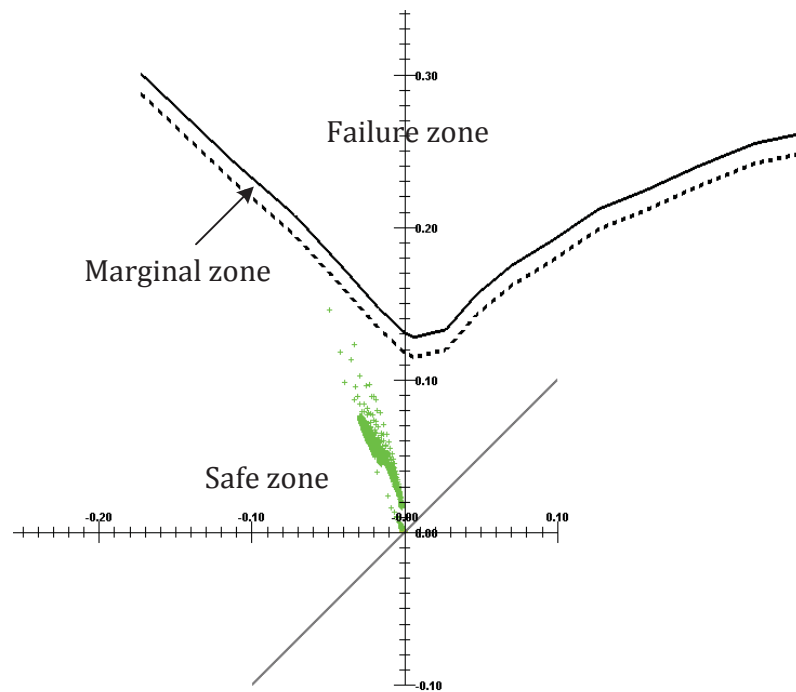
Figure 2.12   FLD quality evaluation for the formed part

The results showed that the difference of springback values with various input design variables is large. To verify the reliability of the simulation, experiments No. 2 and No. 9 in Table 2.3 are selected. Group No.2 represents a relatively best result and No. 9

represents a normal one. The design of the experiment is listed in the Table 2.4. The change of each parameter is set as 50% of its value.

Table 2.4   Experimental Design for Reliability and Sensitivity

Exp. run	x_1 (mm)	v_1 (mm/s)	v_2 (mm/s)	x_2 (mm)	v_3 (mm/s)	Max. Springback value
No.2	2	1.70	8.45	36	7.55	8.63
1A	1	1.70	8.45	36	7.55	14.3
1B	3	1.70	8.45	36	7.55	10.53
2A	2	0.95	8.45	36	7.55	9.15
2B	2	2.65	8.45	36	7.55	10.03
3A	2	1.70	4.23	36	7.55	8.84
3B	2	1.70	12.65	36	7.55	11.13
4A	2	1.70	8.45	18	7.55	19.24
4B	2	1.70	8.45	54	7.55	11.97
5A	2	1.70	8.45	36	3.80	9.24
5B	2	1.70	8.45	36	11.35	9.83
No. 9	16	5.75	6.20	40	2.15	15.35
6A	8	5.75	6.20	40	2.15	17.81
6B	24	5.75	6.20	40	2.15	20.82
7A	16	5.65	6.20	40	2.15	14.74
7B	16	5.85	6.20	40	2.15	14.82
8A	16	5.75	6.10	40	2.15	14.56
8B	16	5.75	6.30	40	2.15	15.3
9A	16	5.75	6.20	38	2.15	17.69
9B	16	5.75	6.20	42	2.15	11.34
10A	16	5.75	6.20	40	2.05	15.12
10B	16	5.75	6.20	40	2.25	16.81

According to these two sets of numerical simulations, it can be easily found that the design variables of x_1 and x_2 are more sensitive compared with v_1, v_2 and v_3,

which can be identified in Table 2.5.

Table 2.5   Springback value change of the sensitivity and reliability simulations

Springback value change	x_1	v_1	v_2	x_2	v_3
No.2	5.67	0.52	0.21	10.61	0.61
	1.9	1.4	2.5	3.34	1.2
No.9	2.46	0.61	0.79	2.34	0.23
	5.47	0.53	0.05	4.01	1.46

It can be found that based on the same percentage change of the design variables, x_1

and x_2 have a relatively higher sensitivity. Small change of their value could result in

the large variation. This phenomenon can be explained as these two values are directly

related to the extension ratio of the deformation and only limited in a special range it

could result a better springback result. It can prove that the parameters for pre-stretch

and additional stretch will influence the final result largely. And the other three

velocities related parameters do not have much effect on the springback value.

2.5.5 Response Surface Setup and Optimal Solution Calculation

According to the previous statement we can realize that the control of springback

value is a really complex problem. There are many parameters need to be considered

and these parameters do not have an explicit relationship to the springback value. From

the initial numerical simulations in previous section it is possible to setup a relationship

between them.

It is huge time consuming to explore each factor relationships. According to the previous simulation, only take two design variables are under consideration, which is the pre-stretch distance and additional stretch distance. Other parameters are determined by the relatively good result in Table 2.3. So in the following further research, three velocities are listed in Table 2.6.

Table 2.6   Values for velocities

$v_1(mm/s)$	$v_2(mm/s)$	$v_3(mm/s)$
1.70	7.10	7.55

The new design variables that we consider are in Table 2.7.

Table 2.7   New design variables

Design Variable	x_1	x_2
Unit	mm	mm

According the previous experiments, still set the constraint as:

$$17.2 \le x_1 + x_2 \le 62.$$

Then employ the experimental design of orthogonal array to simulate again. The design of the experiments is as followed in Table 2.8[5].

Table 2.8   Experimental Design of two-factor five-level

Exp. No.	Factors		Springback value
	x_1	x_2	

1	2	18	16.58
2	5	35	9.49
3	8	22	14.34
4	11	31	9.05
5	14	26	15.39
6	17	27	7.37
7	20	30	10.74
8	23	23	9.52
9	23	34	11.62
10	20	29	8.81
11	17	29	12.86
12	14	35	10.09
13	11	24	7.41
14	8	41	9.82
15	5	19	13.22
16	2	47	8.81

Then, the polynomial equation is employed for curve fitting. It is usually not the case that the higher degree bring a higher accuracy, the degree of 2, 3 and 4 are tried respectively by using Matlab to find the optimum solution, and then compared with the numerical simulation result. The format of polynomial equations of degree 2, 3 and 4 are as followed:

$$f_2 = p00 + p10 \cdot x_1 + p01 \cdot x_2 + p20 \cdot x_1^2 + p11 \cdot x_1 \cdot x_2 + p02 \cdot x_2^2, \quad \text{Eq. 2.17}$$

$$f_3 = p00 + p10 \cdot x_1 + p01 \cdot x_2 + p20 \cdot x_1^2 + p11 \cdot x_1 \cdot x_2 + p02 \cdot x_2^2 \\ + p30 \cdot x_1^3 + p21 \cdot x_1^2 \cdot x_2 + p12 \cdot x_1 \cdot x_2^2 + p30 \cdot x_2^3 \quad \text{Eq. 2.18}$$

$$f_4 = p00 + p10 \cdot x_1 + p01 \cdot x_2 + p20 \cdot x_1^2 + p11 \cdot x_1 \cdot x_2 + p02 \cdot x_2^2 \\ + p30 \cdot x_1^3 + p21 \cdot x_1^2 \cdot x_2 + p12 \cdot x_1 \cdot x_2^2 + p03 \cdot x_2^3 \quad \text{Eq. 2.19} \\ + p40 \cdot x_1^4 + p31 \cdot x_1^3 \cdot x_2 + p22 \cdot x_1^2 \cdot x_2^2 + p13 \cdot x_1 \cdot x_2^3 + p04 \cdot x_2^4$$

The coefficients of polynomial equations for curve fitting are in the Table 2.9.

Table 2.9   Coefficients of polynomial equations

Polynomial Degree	2	3	4
$p00$	7347	-1.323e+05	5.154e+14
$p10$	43.48	639.8	1.085e+13
$p01$	-206.2	3553	-3.479e+13
$p20$	-0.2273	4.984	1.226e+10
$p11$	0.1193	-25.45	-3.661e+11
$p02$	0.9929	-23.6	7.664e+11
$p30$	\	0.01283	-4.718e+08
$p21$	\	-0.09251	1.513e+09
$p12$	\	0.2381	1.887e+09
$p03$	\	-0.004884	-6.052e+09
$p40$	\	\	9.749e+05
$p31$	\	\	-0.0302
$p22$	\	\	-7.799e+06
$p13$	\	\	0.05786
$p04$	\	\	1.56e+07

The optimum point of the response surface of each degree can be calculated in the Matlab. One thing that needs to be careful is that the objective is to find the absolute minimization value of the objective function since the objective function represents the springback value and it approaches to zero.

Set the polynomial equation of degree 2 as an example to verify the optimization solution is global and robust, it could be checked with different initial points. The result is listed in the Table 2.10.

Table 2.10   Optimization result with different initial points of polynomial equation of degree 2

Initial Point	x_1	x_2	fval
[50, 40]	12.5282	30.0591	1.05914
[40, 30]	12.3254	30.5510	0.1810
[2, 65]	12.3254	30.5510	0.1810
[25, 25]	12.3254	30.5510	0.1810
[70, 15]	9.7000	30.7681	19.0917
[65, 2]	12.3254	28.5510	0.1810

From the above table, it seems that four of the initial points reached a local minimum point. However, other initial point further improves the optimization result and the value of 0.1810 is good enough for a spring back value.

For the other two cases, use the same method and verify with the different initial point. The results are listed in Table 2.11.

Table 2.11   Local minimum point of the polynomial equations

Degree	2	3	4
x_1	12.3254	12.0462	12.4871
x_2	30.5510	31.5474	32.5473
fval	0.1810	3.5741	7.2671

Due to the accuracy of the polynomial equation for different degrees, different optimum points and the optimization results are shown. However, to further investigate the final result we need to run the FEA software for numerical simulation again for result verification. Run the FEA simulation by employing the optimum point [12.33, 30.55], it could be seen from Figure 2.13 that the maximum springback on the formed panel is around 5.16mm. The result showed that this optimization result fits well with the simulation.
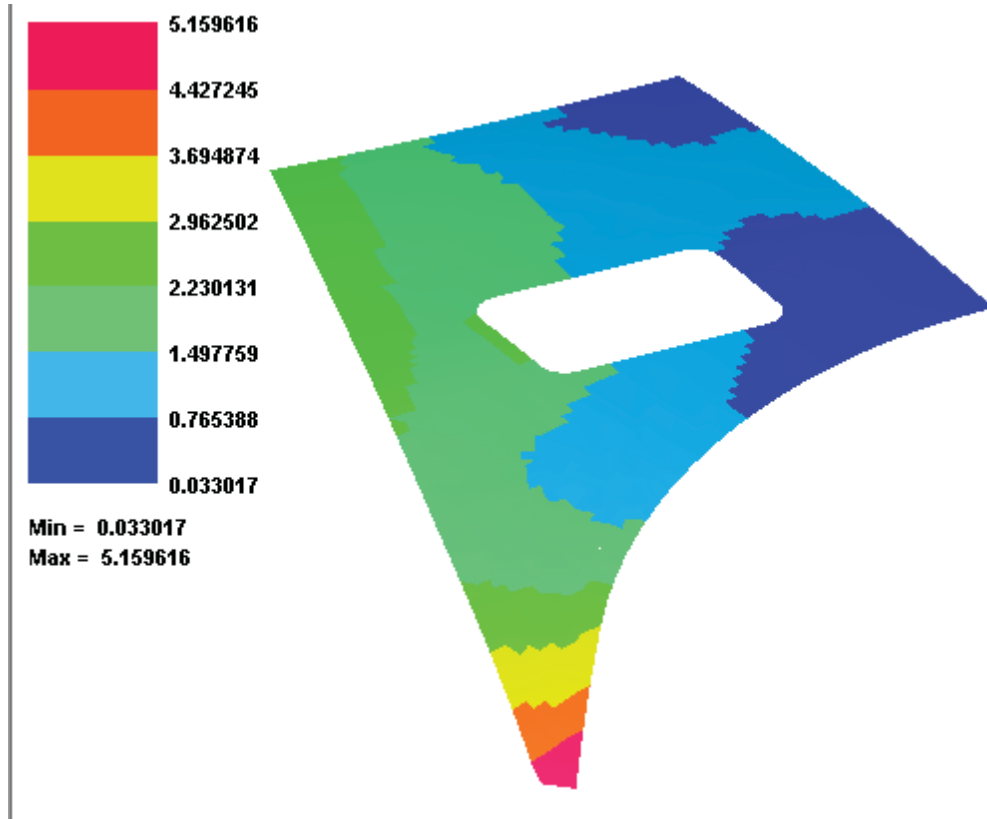
Figure 2.13   Optimum point of optimization result verification in Pam-Stamp

CHAPTER 3   POCKETS POSITION DESIGN ON FLAT

BLANK SHEET

3.1 Introduction

In order to achieve sheet metal forming process, the influences of a considerable number of process parameters are evaluated experimentally or analytically. For the case in this study that the pockets are machined before the stretching, besides the parameters of the process, manufacture condition, the blank design also plays an important role in the determination of the quality of the panel, especially for the accuracy of the pockets shape and position. To reduce the factors that taken into consideration, the loading trajectory of the jaws needs is calculated first, and then with this determined stretch forming process, conduct FEA simulation, analyze result, make modification and finally get the designed flat blank.

In this study, design of pockets on the blank is studied based on the shape sensitivity method. The blank design procedures could be described as the following flowchart in Figure 3.1. Based on the designed CAD model of the aircraft panel, an initial blank with pockets is assumed. Then this initial blank is used to perform stretch forming

process to obtain the CAD data of the formed panel. Based on the deviation compared between the formed panel with the designed panel, modify the assumed initial blank and conduct the FEA simulation for the next iteration. If the result of the comparison shows that difference is less than the tolerance, the design procedures is finished and the blank could be machined for stretch forming. If the difference exceeds the tolerance, make modification for another iteration until it meets the requirement.
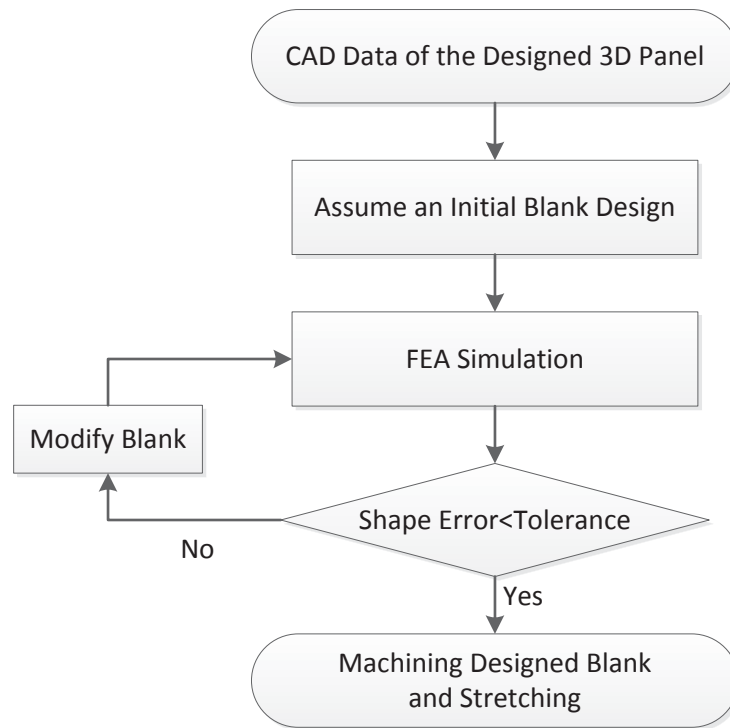

Figure 3.1   Blank design procedures flowchart

3.2 Blank Design for Aircraft Skin with Simple Pocket Features

Based on the designed 3D panel, the blank is employed for conducting the stretch

forming process. Due to the thin thickness of sheet metal, which usually around $2mm$ to $3mm$, in the pocket location design, the sheet metal is treated as a surface and the pocket as the spline curve on the surface. When the geometry information is imported into FEA simulation software, the thickness attribution would be taken into consideration for deformation analysis. In this section, a designed panel with single curvature, as Figure 3.1 shows, is set as an example.

Blank thickness: 2.4mm
Pocket thickness: 1.9mm
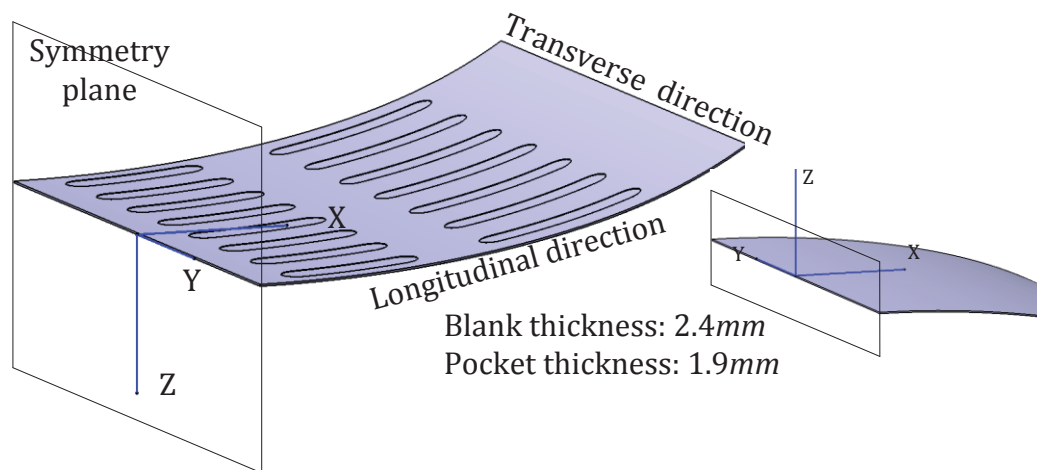
Figure 3.2   Designed panel with simple features

3.2.1. Initial pocket position assumption

The method applied for initial blank design is unfolding. For single curvature surface, it could be regarded as a ruled surface of degree $1 \times n$, which means that the surface was created by sweeping a linear profile (of degree 1) along a guide of degree n.

Figure 3.3 showed the front view of unfolding process for a single curvature surface. The arc length of the designed panel profile is equal to the length of the unfolded profile. The profile of the designed panel could be described by the polynomial function as:

$$z = p_1 \cdot x^3 + p_2 \cdot x^2 + p_3 \cdot x + p_4.$$ Eq. 3.1
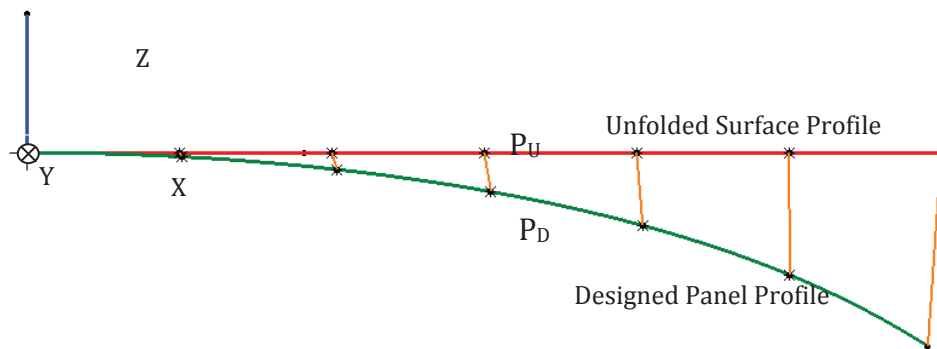
Figure 3.3   Illustration of single curvature panel unfolding

After unfolding, the curved surface is transferred onto the flat surface. Considering that in the whole stretch forming process, it usually has at least 2% extension ratio in the longitudinal direction, the arc length of the designed panel would be 2% more than X axis value in the initial blank design. For the Y axis, it is assumed that the length in transverse direction does not change. Figure 3.4 shows the procedures for obtaining the initial pockets position.
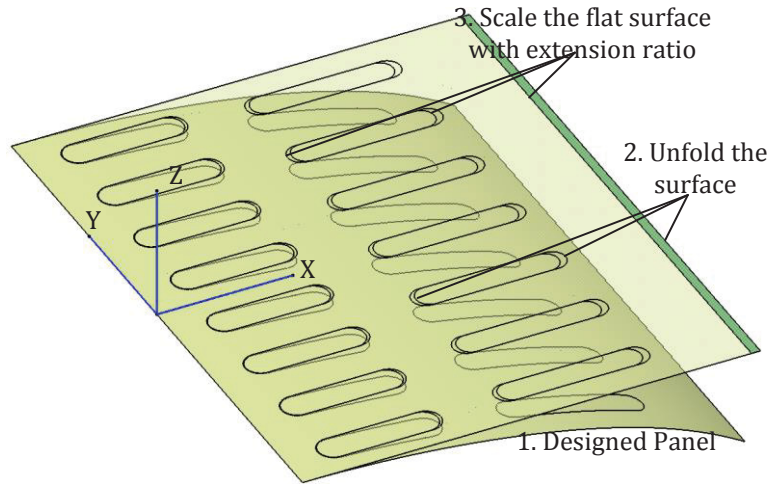
Figure 3.4 Procedures for the obtaining the initial pockets position

The transformation matrix for the initial pockets position is calculated by the following equations:

$$\left. \begin{array}{l} \int_{0}^{x_D} \sqrt{1+\left(\dfrac{dz}{dx}\right)^2}\, dx = \left(1+2\%\right)x_U \\[2mm] y_D = y_U \\[2mm] z_U = 0 \end{array} \right\} \Rightarrow tran(x,y,z), \qquad \text{q. 3.2}$$

and thus the unfolded surface could be obtained by

$$\begin{pmatrix} x_U \\ y_U \\ z_U \end{pmatrix} = tran(x,y,z) \begin{pmatrix} x_D \\ y_D \\ z_D \end{pmatrix}. \qquad \text{Eq. 3.3}$$

3.2.2. Initial blank outline determination

Based on the above discussion, the initial position of the pockets could be

obtained. However, the outline of the blank still needs further study. A proper outline of

the blank could largely improve the problem of stress concentration due to the pockets

machined before stretching and also the over thinning around the pockets area, which

could reduce the possibility of the potential defects. As we can see in Figure 3.5, the

blank is stretched without additional outline compensation and extension ratio in the

longitudinal direction is 5.58%, in the transverse direction, the blank shrink to the length

less than the desired, which could reach to the ratio of 3.52% compared with the design

panel.
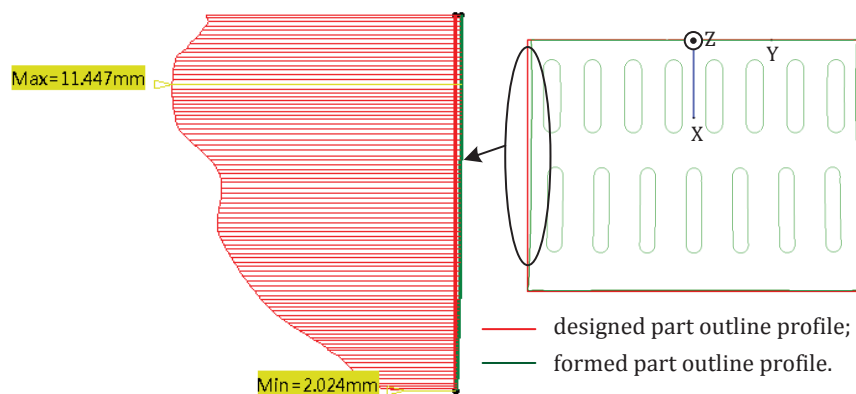

Figure 3.5   Deformed part without outline compensation

For the pockets and their around areas, the thickness distribution, as Figure 3.6 shows, is

not uniform enough although part of them have reached the designed thickness as

shown in Figure 3.2. All the problems mentioned above could count as defects and they

need to be eliminated or reduced by the means of proper outline design.

Thickness of the
deformed pockets

Thickness of the
deformed part
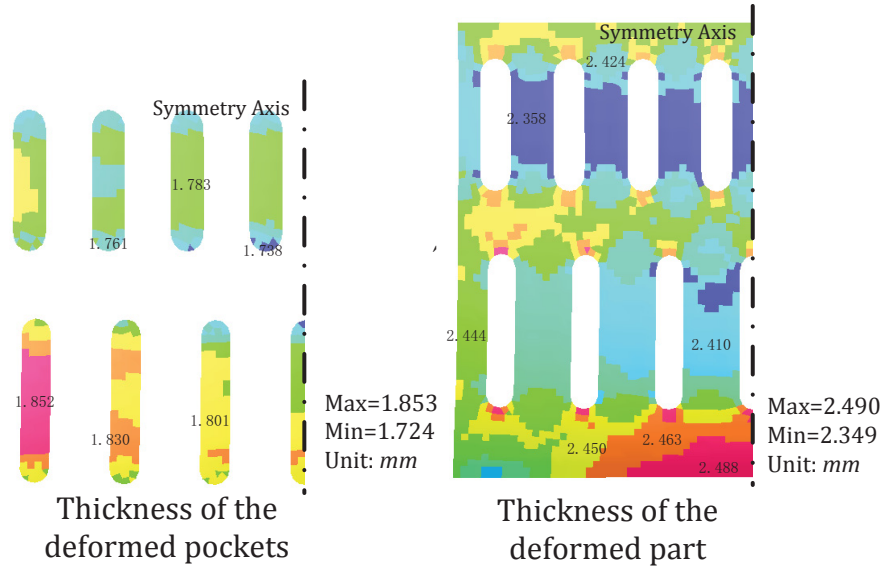
**Figure 3.6   Thickness distribution of the deformed part without outline compensation**

To determine the outline of the blank, basically it could be done by increasing the

length in transverse direction, in longitudinal direction or partial compensation around

the pockets area as Figure 3.7, Figure 3.8, Figure 3.9 show.
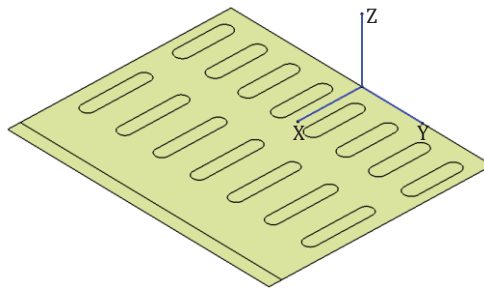
Figure 3.7   Blank outline design methods - compensation in transverse direction
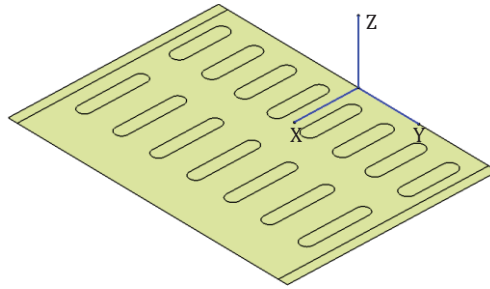
Figure 3.8   Blank outline design methods - compensation in longitudinal direction
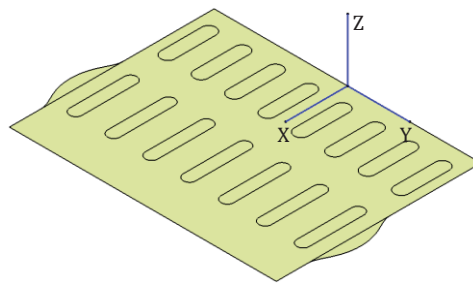
Figure 3.9   Blank outline design methods - partial compensation

For each method of compensation, they have their own functions to improve the quality

of the panel. Like the compensation in transverse direction, it could improve the

springback distribution at the end part of the panel and the compensation in

longitudinal direction and the partial area could reduce the problem of stress

concentration and nonuniform thickness distribution. Combination of these

compensation methods could achieve a better result.

However, there is no specific rule to define how exact these boundaries of the

panel are working. The basic method to find the most appropriate boundaries is by

trying different ways. Too large length compensation would result in material waste and too small compensation could not solve the quality problems mentioned above. For the method of partial compensation, although it could improve the quality of the panel in some degree, it increases the workload of outline machining. And also, by designing the appropriate length of compensation in transverse and longitudinal directions, it could also achieve the same result.

3.2.3 Shape Deviation Evaluation

After finishing FEA simulation, the result of formed panel could be accessed and analyzed. In this section, the formed panel of simulation result and the designed panel would be compared and evaluated under the same coordinate system. From the previous analysis it is known that the thickness distribution and the extension ratio have all met the requirements. Especially for the small springback value, it means that the curvature of the whole part fits the designed panel well, so the thing we need to take into consideration is the location of the pockets.

To precisely determine the deviation between the designed panel and the formed panel, the comparisons in X, Y, Z axes are applied. First for deviation in Z direction, go to the front view of the 3D panel, it can be seen from Figure 3.10. As long as the formed

panel has a small springback value in Z direction within the tolerance, the shape deviation in the Z axis could be regarded qualified.
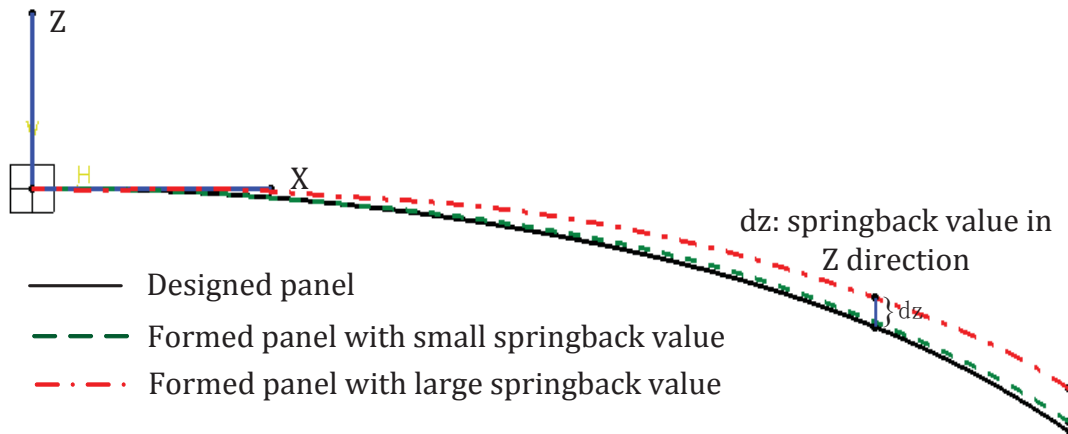
Figure 3.10   Illustration of springback value in Z direction

The next thing needs to be considered is the deviation in the X and Y directions. Based on the designed panel and the panel formed by simulation, extract the boundaries of pocket profiles since we only need to consider the accuracy of the profiles boundary, then project these two profiles onto XY plane and combine them under same coordinate system, as shown in Figure 3.11. The one generated by the projection of designed panel is set as the reference to check the shape deviation of the formed panel in X and Y directions.

Pocket profiles of designed panel   Pocket profiles of formed panel

Combination of these two profiles under one coordinate
system and project the profiles on XY plane
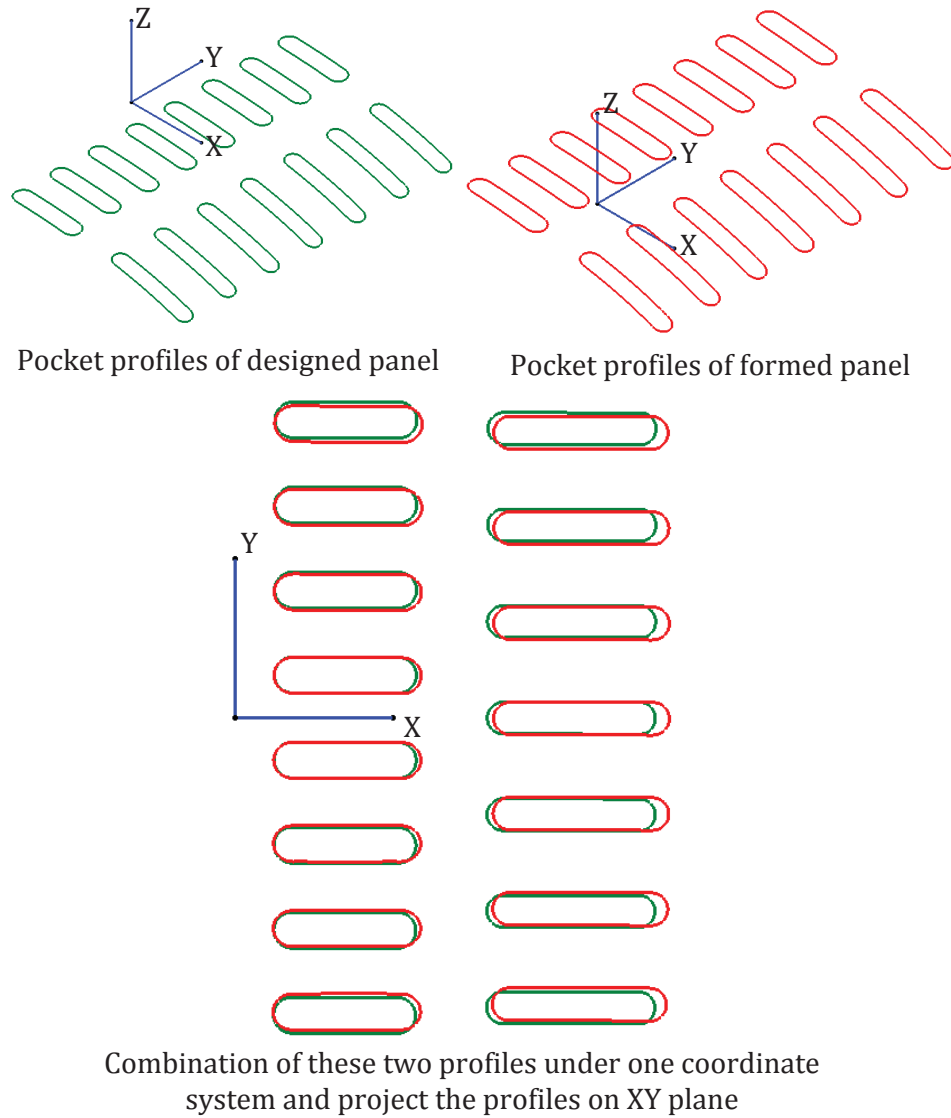
Figure 3.11   Comparison of the deformed profiles of the initial blank design and

target profiles

Based on the comparison between the projection of the formed part and the designed

skin part on XY plane, the deviation of each pocket profile could be evaluated. It could

be illustrated as shown in Figure 3.12.
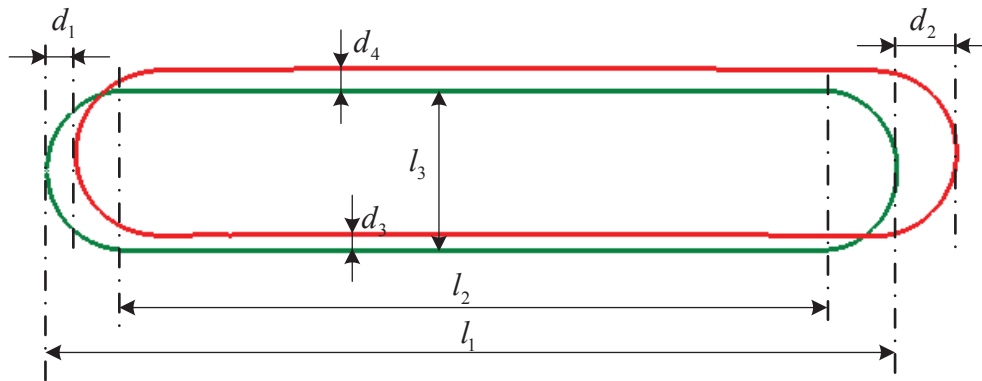
Figure 3.12   Illustration of the parameters to define the deviation in X and Y direction

In Figure 3.12, l_1, l_2, l_3 represent the parameters of reference pocket, d_1, d_2 d_3

and d_4 indicate the deviation between the reference profile and the formed profile.

3.2.4 Modification of Blank Design

From last section, the parameters to evaluate the deviation of simple pocket shape

have been obtained. When designing the initial blank by unfolding the pocket surface

onto the XY plane, as Figure 3.13 shows, parameters of s_1, s_2, s_3 and R are

employed for the further blank design modification purpose.
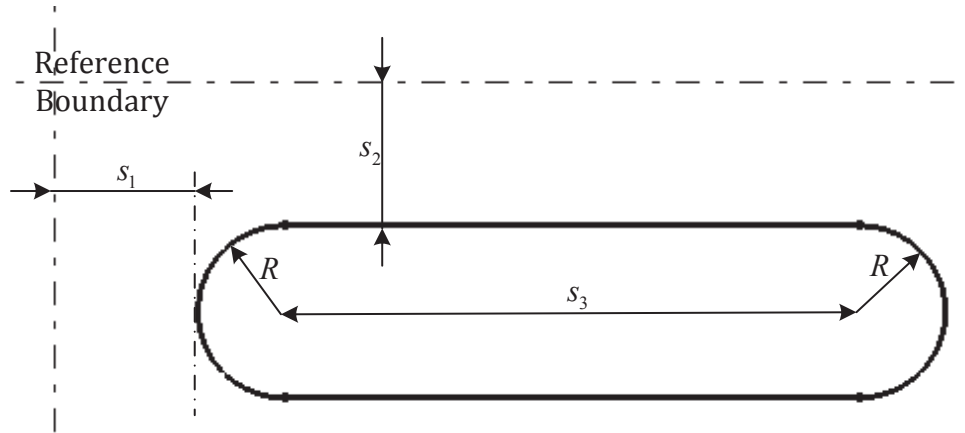
Figure 3.13   Design parameters of pockets on flat blank

By using the deviation evaluated in Figure 3.12, the parameters for blank design could be updated as equations:

$$s_1^{'} = s_1 - d_1,$$

<div align="right">Eq. 3.4</div>

$$s_2^{'} = s_2 + d_4,$$

<div align="right">Eq. 3.5</div>

$$s_3^{'} = s_3 - \left(d_2 - d_1\right),$$

<div align="right">Eq. 3.6</div>

$$R^{'} = R - \frac{d_4 - d_3}{2}.$$

<div align="right">Eq. 3.7</div>

Based on the updated blank design, under the same condition of stretch forming process and material properties, conduct another simulation of the stretch forming, evaluate the deviation and make the modification until it meets the requirement.

3.2.5 Simulation Result

Due to the simple shape of the pocket and the symmetry part only has single

curvature, after four iterations, it has reached the deviation requirement. Figure 3.14

showed the changing of pocket profiles in these four iterations.
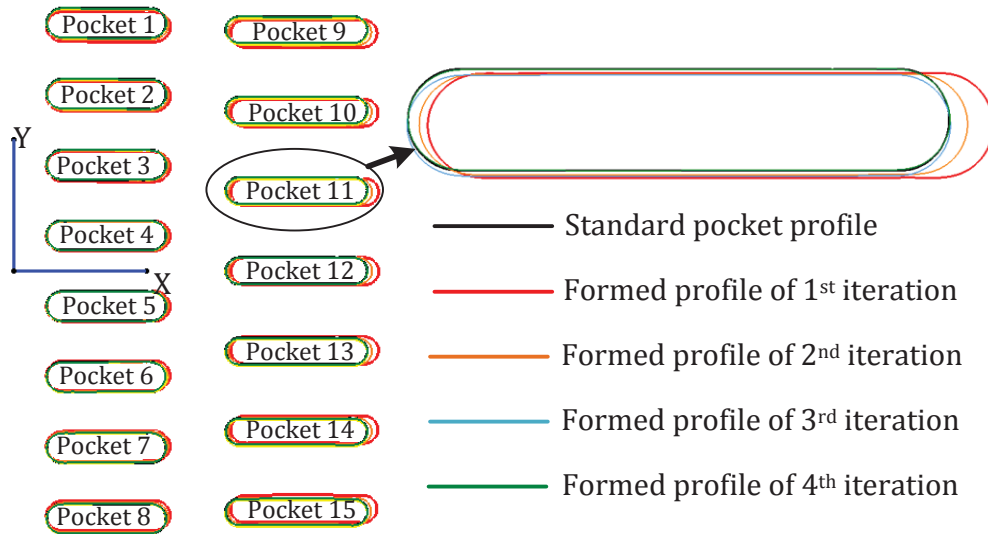
Figure 3.14   Pocket profiles in four iterations

Table 3.1 is the list of the deviation of each pocket profiles with its corresponding

target profile. In the first four iterations, the deviation has decreased largely. For the fifth

iteration, it stayed around the same level of fourth iteration, even some of the pockets

rebounded.

Table 3.1   Pockets deviation with the target profile in four iterations

Max. deviation (*mm*)	Iteration 1	Iteration 2	Iteration 3	Iteration 4	Iteration 5
Pocket 1	8.863	3.899	0.726	0.952	1.16
Pocket 2	7.049	3.944	1.036	0.857	0.801
Pocket 3	6.73	3.235	1.083	0.871	0.736
Pocket 4	6.083	3.177	1.027	0.689	0.661
Pocket 5	6.02	3.093	1.081	0.729	0.65
Pocket 6	6.35	3.078	1.231	1.148	1.53
Pocket 7	6.561	3.547	0.911	0.871	0.815
Pocket 8	7.621	3.454	1.188	1.047	1.166
Pocket 9	15.986	6.783	2.342	1.128	0.932
Pocket 10	16.911	7.714	2.4	0.596	0.633
Pocket 11	17.439	7.396	2.568	0.541	0.587
Pocket 12	17.566	7.387	0.812	0.741	0.577
Pocket 13	17.257	7.169	2.755	1.271	0.609
Pocket 14	16.525	6.677	2.894	0.599	0.678
Pocket 15	15.4	6.07	3.061	1.101	0.967

From this case, it can be concluded that this method could be used for the blank design. However, the accuracy cannot meet the requirement even for this simple case. Method for higher accuracy needs proposed.

3.3 Blank Design for Aircraft Skin with Complex Pocket Features

However, in the real industry, the shapes of the pocket are not simple like the case mentioned above. The panel that used for assembly in aircraft shown in Figure 3.15 is provided by Bombardier Inc. It can be identified that the shapes are irregular and when

trying to make the deviation evaluation and flat blank design modification, it cannot be

achieved by just employing just several parameters. For the size of the designed part is

shown in Figure 3.16.
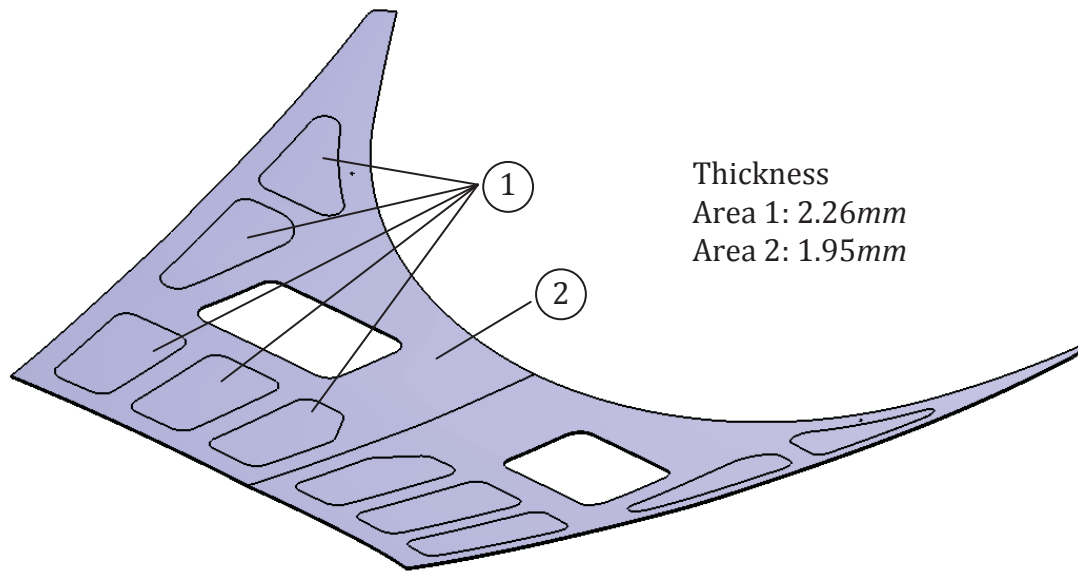
**Figure 3.15   Designed panel of double curvature with complex features**
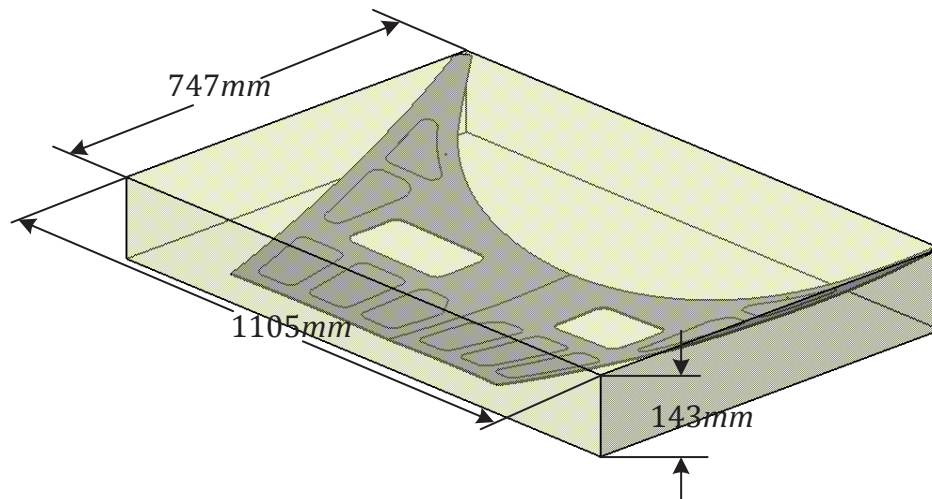
Figure 3.16   Size of the designed part

To solve this problem, a new approach is proposed by dispersing the pocket profiles to analyze the profile and evaluate the deviation, and then the shape sensitivity method is employed to improve the blank design. Since this panel is designed with symmetry structure, the following research is all done with half part.

3.3.1 Initial Blank Design

Unlike the panel with single curvature that can be regarded as a ruled surface of degree $1 \times n$, the double curvature panel cannot be unfolded onto a flattened surface without length distortion. With the assistance of CATIA unfolding function, the double curved surface is unfolded onto the XY plane. The length distortion distribution is shown in Figure 3.17, which is along X direction with the reference of YZ plane. It could be observed that the length distortion is very small compared with the value of shape deviation and it could be compensated in the future modification.

| 0.197 % |
| 0.148 % |
| 0.099 % |
| 0.049 % |
| 1.164e-008 % |
| -0.049 % |
| -0.099 % |
| -0.148 % |
| -0.197 % |

Maximum: 0.15295%
Minimum: -0.19718%
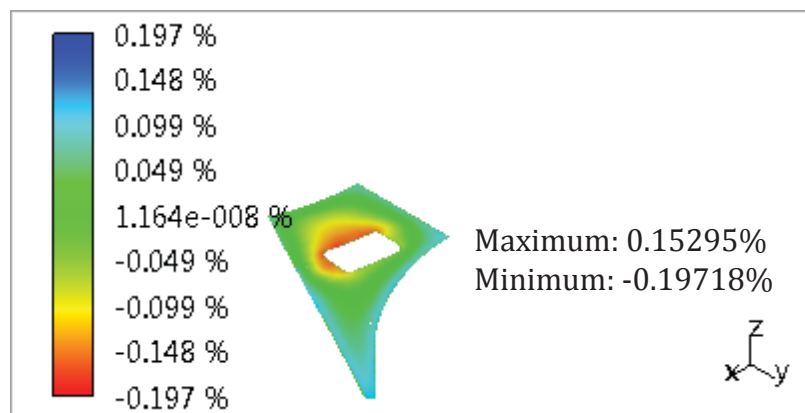
Figure 3.17   Flattened surface length distortion

By using this unfolding function, the position of initial pockets could be determined as

Figure 3.18 shows. The outline of the initial blank is adjusted for first process simulation

as $1620mm \times 900mm$, as Figure 3.19 shows.

Symmetry plane

Z

X

Y

Unfolded pocket
profile on XY plane

Designed Pocket
Profile
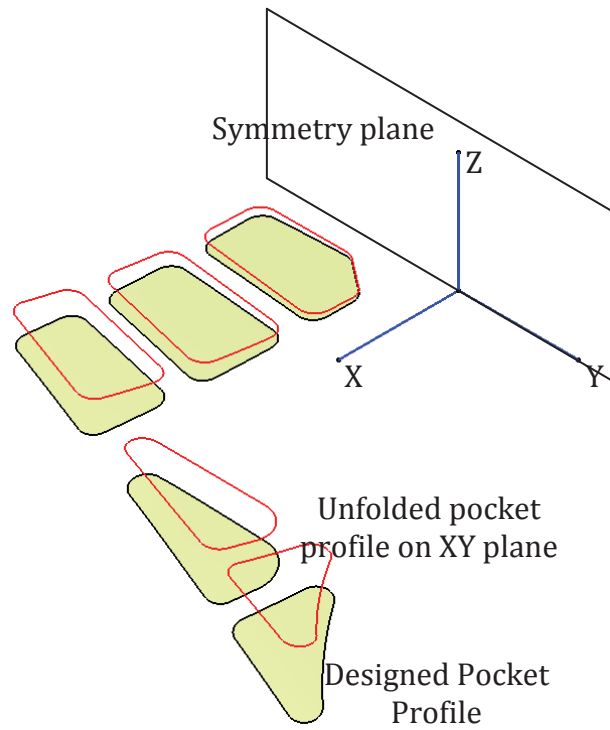
Figure 3.18   Initial pockets position determination for double curvature panel
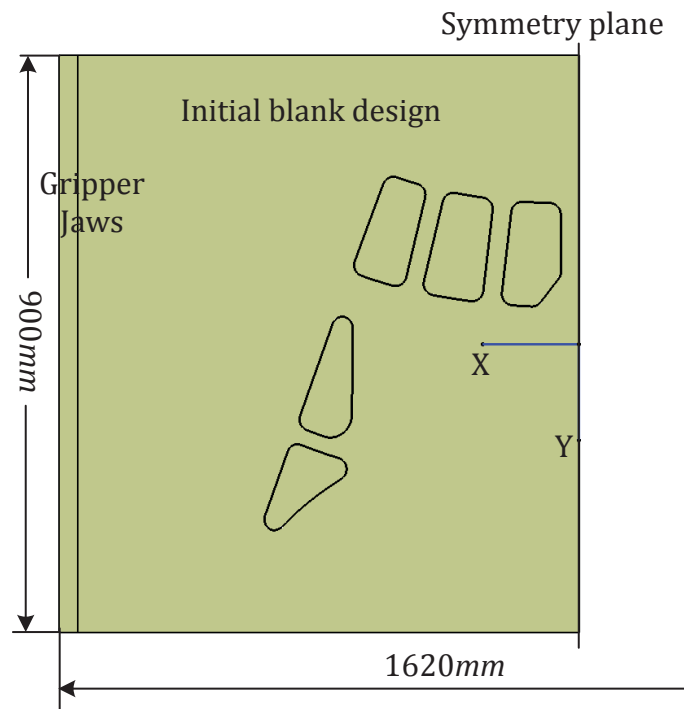
Figure 3.19　Dimensions of initial blank design

3.3.2 Shape Deviation Evaluation of the Formed Part

After the initial designed blank undergoes the process of wrap forming, additional stretch, trimming and springback, the first formed part is obtained. First we need to check the springback value in Z direction. Figure 3.20 shows that most area of the panel is less than 3mm, which has met the requirement.
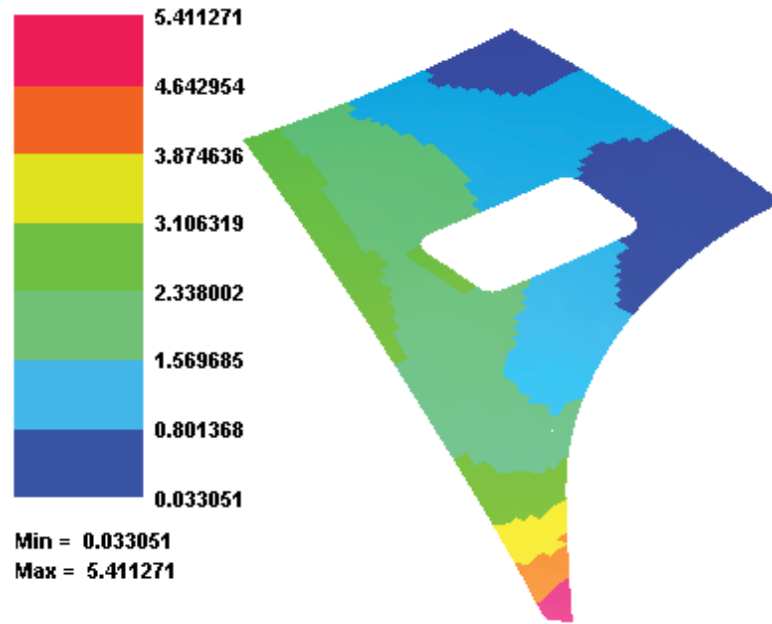
Figure 3.20   Springback value distribution in Z direction

For the deviation in X and Y direction, project the standard profiles and formed pocket profiles in XY plane as shown in Figure 3.21. It could be observed that for the deviation between the formed profile and the standard profile, due to the irregular shape, it is hard to employ just a few parameters to define the deviation.
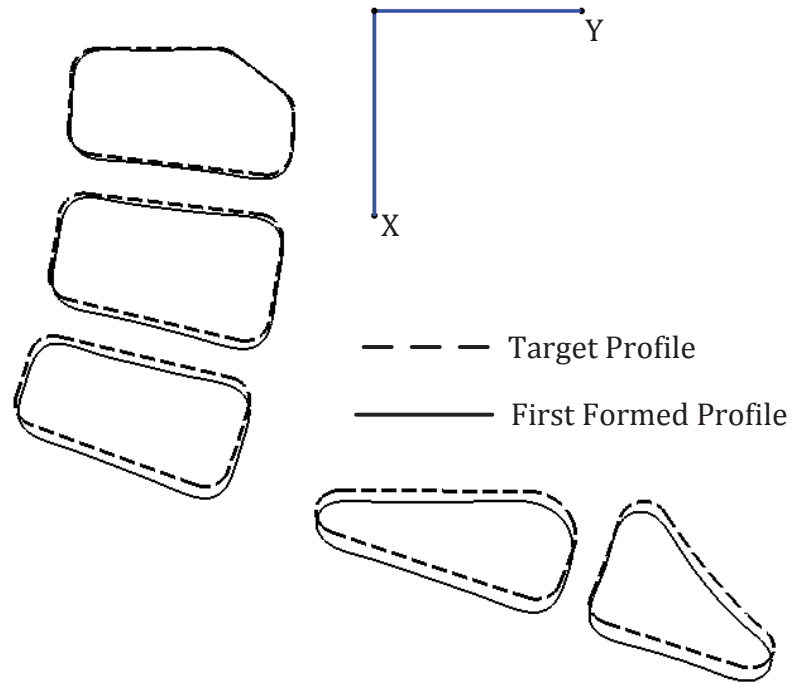
Figure 3.21 **Comparison of pocket profiles between the deformed profiles after first**

iteration and target profile

To solve this issue, the method of dispersing the profiles into numerous points is employed. The correspondence relation between the standard profile points and the formed profile points could be found by reading the mesh information since during the FEA simulation, the mesh keeps unchanged as Figure 3.22 shows.
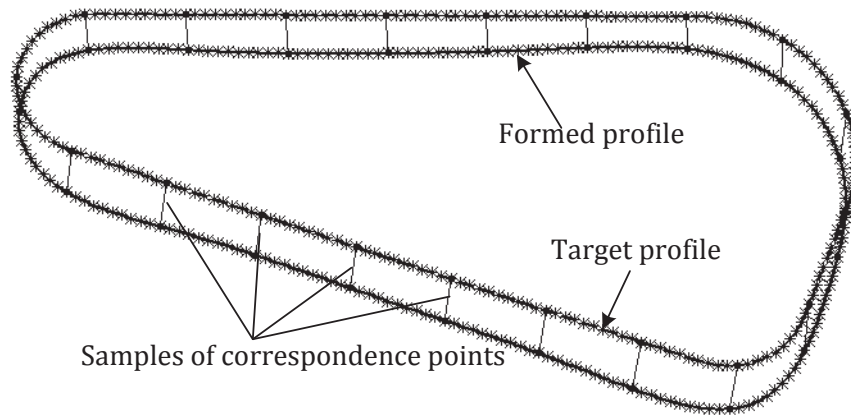
Figure 3.22   Profiles dispersing and correspondence relationship setup

Then reading the coordinates of the dispersed points, the deviation is evaluated by calculating the coordinate difference in X and Y direction respectively.

3.3.3 Blank Design Modification by Sensitive Method

The blank design could be improved based on the deviation evaluation in the previous sections. In this section, the shape sensitive method is employed. As shown in Figure 3.23, P_D represents the one of the node position on pocket profile of the initial designed blank. P_F represents the correspondence node after deformation. P_T represents the node position on the target contour.
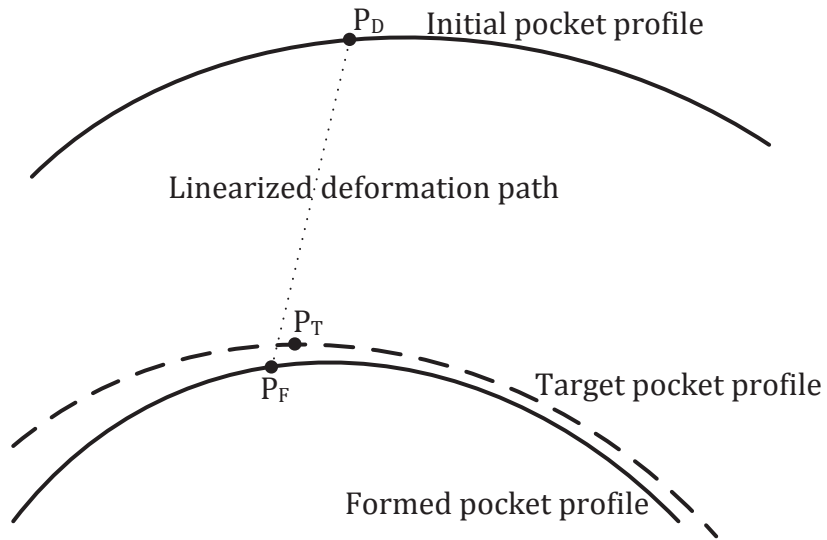
Figure 3.23   Movement of node in deformation process

When the blank deformation finished, the offset of blank is determined by the shape sensitivity. As Figure 3.24 and Figure 3.25 show, P_D^{n-1} and P_D^{n} indicate the node of designed blank in $(n-1)$th and nth design. P_F^{n-1} and P_F^{n} indicate the node of formed part after $(n-1)$th and nth deformation. Vector $P_D^{n} - P_D^{n-1}$ is found as the blank offset and $P_F^{n} - P_F^{n-1}$ as deformation offset of each node.
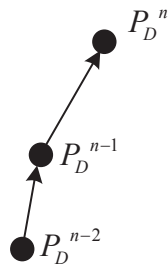
Figure 3.24   Node on designed flat blank
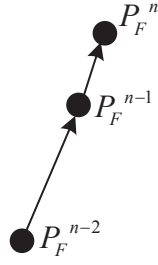
Figure 3.25   Node on deformed panel

Then the sensitivity factor could be defined as how much the blank design offset will influence the formed profile shape, as the equation:

$$S^n = \frac{\left|P_D^{\ n} - P_D^{\ n-1}\right|}{\left|P_F^{\ n} - P_F^{\ n-1}\right|}.$$ Eq. 3.8

The new designed blank could be derived as

$$P_D^{\ n+1} = P_D^{\ n} + S^n \cdot \delta^n,$$ Eq. 3.9

where δ represents the shape deviation between the formed pocket profile and the target pocket profile. Since the deviations are all based on the X and Y direction respectively, so the updated blank design also should be considered in X and Y direction as

$$P_D^{\ n+1}\Big|_X = P_D^{\ n}\Big|_X + S^n\Big|_X \cdot \delta^n\Big|_X$$ Eq. 3.10

and

$$P_D^{\ n+1}\Big|_Y = P_D^{\ n}\Big|_Y + S^n\Big|_Y \cdot \delta^n\Big|_Y.$$ Eq. 3.11

3.3.4 Simulation Results Comparison and Analysis

Figure 3.26 shows numbering of the five pockets profiles in six iterations and Figure 3.27 amplifies for the detail of pocket 5.
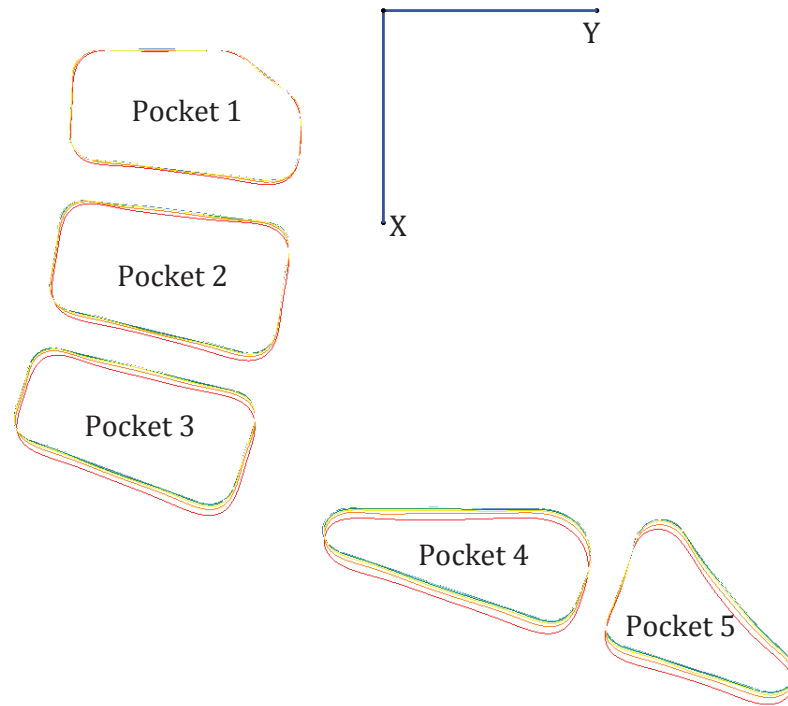
Figure 3.26   Numbering and six iterations of five pocket profiles
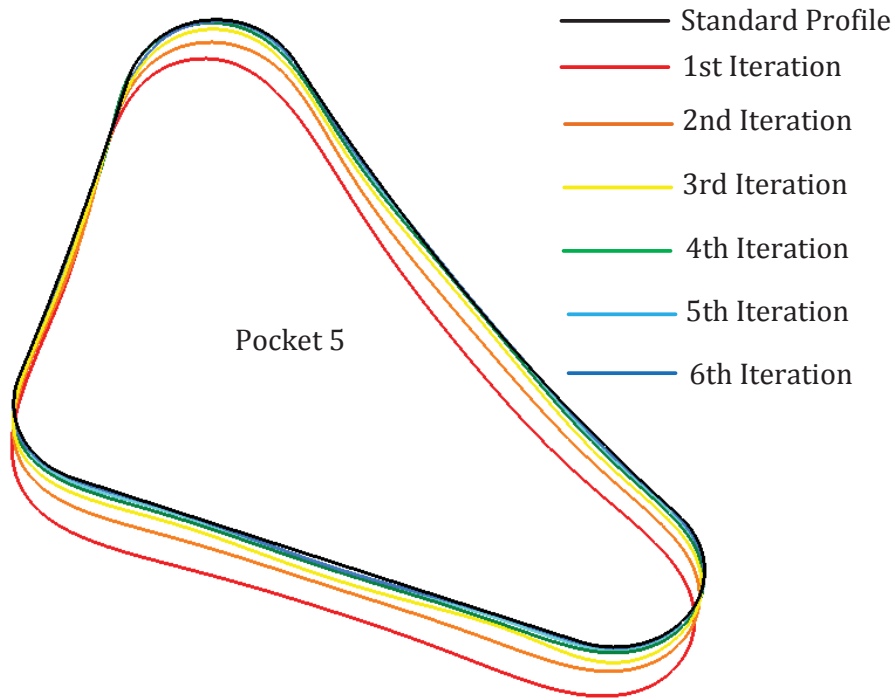
Figure 3.27   Iteration comparison of pocket profile 5

Table 3.2 is the list of maximum deviations between the formed profiles and the target profiles on XY plane by using the sensitivity method. After five iterations, the deviation could be decreased to around 0.2*mm* to 0.3*mm*. In the sixth iteration, it is floating around that level. Since the sensitive method requires the two offset blank, the sensitive factor for second blank design is set as 1, which means

$$P_D^{\ 2}\Big|_X = P_D^{\ 1}\Big|_X + \delta^1\Big|_X \qquad\qquad \text{Eq. 3.12}$$

and

$$P_D^{\ 2}\Big|_Y = P_D^{\ 1}\Big|_Y + \delta^1\Big|_Y. \qquad\qquad \text{Eq. 3.13}$$

From Table 3.2 we can also see that from the first iteration to the second, the deviation decreased most. For the following iterations, their convergence rates slow down since they almost reached the target profile.

Table 3.2   Maximum deviations between the formed profiles and the target profiles on XY plane by using the sensitivity method

Max. deviation (*mm*)	Profile 1	Profile 2	Profile 3	Profile 4	Profile 5
Iteration 1	3.646	6.629	8.922	10.71	10.506
Iteration 2	1.932	2.25	2.275	2.191	2.704
Iteration 3	0.817	0.611	0.77	1.139	0.994
Iteration 4	0.717	0.386	0.349	0.831	0.557
Iteration 5	0.23	0.245	0.221	0.372	0.314
Iteration 6	0.253	0.217	0.318	0.367	0.348

Table 3.3   Setting the sensitive factor as 1 in all the iterations

Max. deviation (*mm*)	Profile 1	Profile 2	Profile 3	Profile 4	Profile 5
Iteration 1	3.646	6.629	8.922	10.71	10.506
Iteration 2	1.932	2.25	2.275	2.191	2.704
Iteration 3	0.842	1.074	1.554	0.981	1.001
Iteration 4	0.624	0.767	0.684	1.109	0.667
Iteration 5	0.781	0.631	0.66	0.812	0.752
Iteration 6	0.507	0.63	0.774	0.608	0.512

To prove the effective of the sensitivity method, Table 3.3 shows the result of setting the sensitive factor as 1 in all the iterations. The results of first two iterations

should be the same as the sensitive method. In the following iterations, it could be

found the values of maximum deviation always floating around 0.5mm to 0.6mm, that is

to say that the sensitive factor 1 is no longer suitable when the deviation has reached a

certain level.

The Table 3.4 listed the case of setting the sensitive factor as 0.5 during all the

iterations of blank design. For the final result, it showed that it could reach to the level

of around 0.2mm to 0.3mm. However, it experienced 11 iterations to get the same level

as the sensitive method.

Table 3.4   Setting the sensitive factor as 0.5 in all the iterations

Max. deviation (mm)	Profile 1	Profile 2	Profile 3	Profile 4	Profile 5
Iteration 1	3.646	6.629	8.922	10.71	10.506
Iteration 2	2.124	3.36	4.552	5.346	5.506
Iteration 3	1.167	1.833	2.381	3.131	3.077
Iteration 4	0.872	1.127	1.554	1.823	1.542
Iteration 5	0.57	0.978	0.97	1.035	1.157
Iteration 6	0.506	0.591	0.568	0.794	0.917
Iteration 7	0.399	0.484	0.511	0.433	0.61
Iteration 8	0.437	0.437	0.404	0.32	0.345
Iteration 9	0.383	0.362	0.373	0.744	0.24
Iteration 10	0.407	0.375	0.317	0.364	0.294
Iteration 11	0.295	0.461	0.374	0.294	0.338

Based on the three cases talked above, that the sensitive method, keeping the

sensitive factor as 1 and 0.5 during all the iterations, it could be found that applying the

sensitive method to the blank design could not only result in a relatively good result but also it largely decrease the numbers of iteration.

3.3.5 Quality of the Deformed Part and Analysis

Since the springback phenomenon is considered in the deviation in Z direction, the quality of the deformed part will be focused on the thickness distribution, FLD evaluation and possible reason for deviation.

The thickness distribution of the deformed part is shown in Figure 3.28 and Figure 3.29. From them it could be seen that although some of the places are not fully stretched or over thinning, the maximum thickness difference with the target value is around $0.04mm$ for area 1 and the $0.025mm$ for area 2.
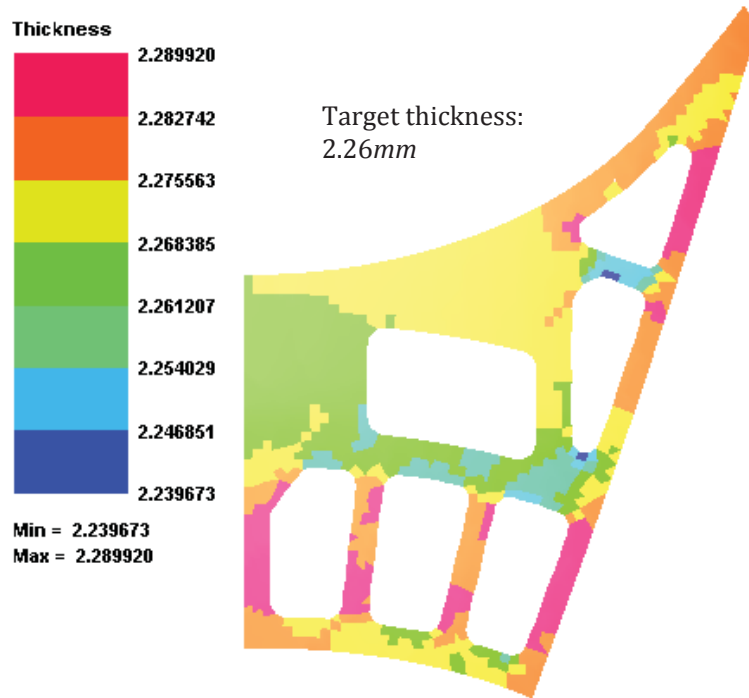
Figure 3.28   Thickness distribution of the deformed part area 1
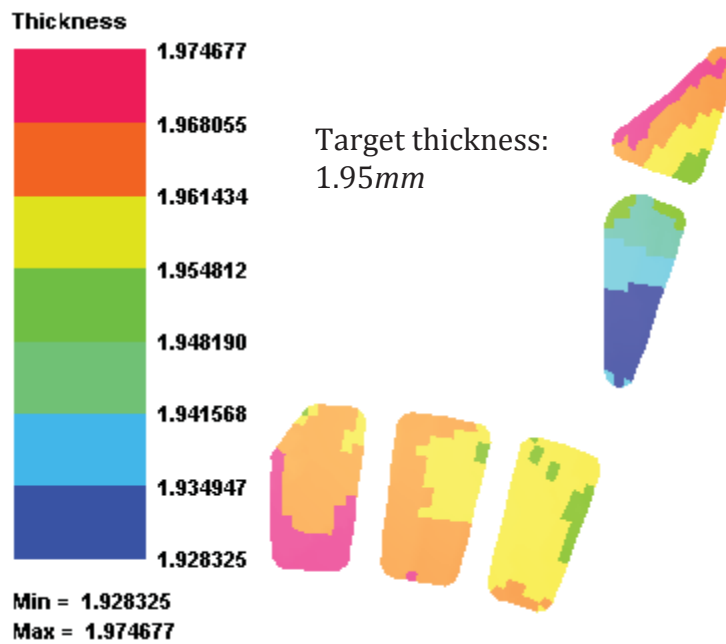
Figure 3.29   Thickness distribution of the deformed part area 2
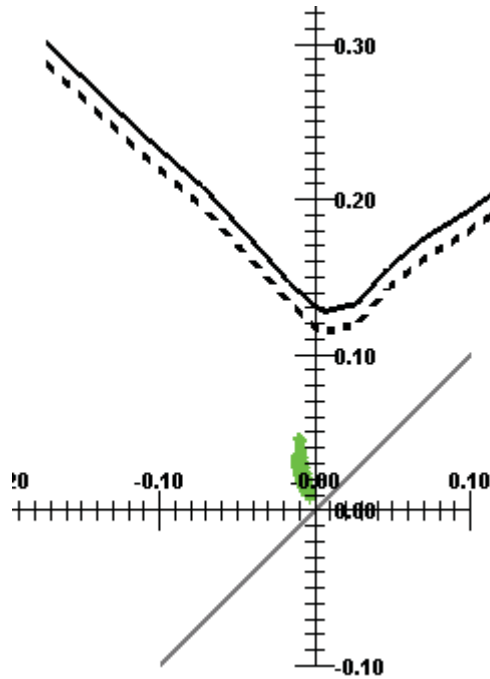
Figure 3.30   Quality evaluation of the deformed part

The Figure 3.30 shows the quality evaluation of the deformed part by FLD curve. All the points are located in the safe zone.

Another thing that needs to be mentioned here is the possible reason of the deviation keeps around $0.2mm$ to $0.3mm$. Except the accuracy of simulation and the blank design in FEA simulation, due to the thin thickness, the blank is meshed as a surface with triangle and quadrangle, whose boundaries are straight lines, as shown in Figure 3.31. The shape deviations δ are unavoidable because of the space between the straight line and the spline curve.
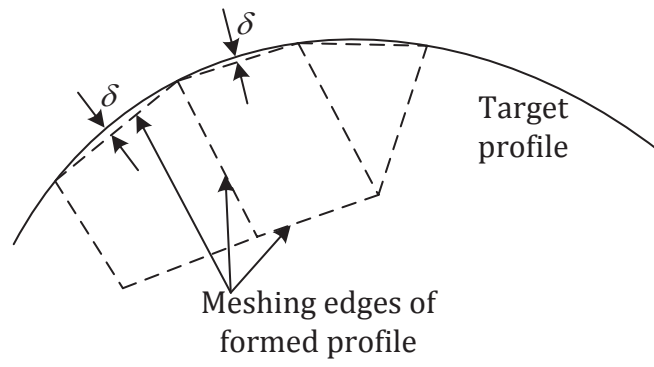
Figure 3.31   Shape deviation caused by the meshing edges

CHAPTER 4   APPLICATIONS

In this chapter, two examples were studied for the reliability and feasibility of this method.

4.1 Example 1

To verify the feasibility and reliability of the sensitivity method for flat blank design, a more complex part is employed in this example. Basically it keeps the pocket features in CHAPTER 3 , an additional pocket is designed as Figure 4.1 shows, in which the thickness information also could be found. The size and dimensions are same as the example in Section 3.3.

The way for initial blank assumption is same like the method mentioned in Section 3.3.1. However, from Table 3.2 it could be found that, based on the first assumption, the deviation of first iteration result is relatively large compared with the following iterations. To investigate the component of deviation, as Figure 4.2 shows, it is mainly in Y direction. So in the assumption of initial blank and pocket position for the case of example 1, the extension ratio is set as 3%. The result from Table 3.2 and Table 4.2 shows that for the deviation of profile 3, profile 4 and profile 5 after first iteration, it has largely decreased.

For the deviation of other profiles, it stays at the same level since the deviation also

could be caused in X direction.

Thickness:
Area 1: 2.25mm
Area 2: 2.05mm
Area 3: 1.85mm
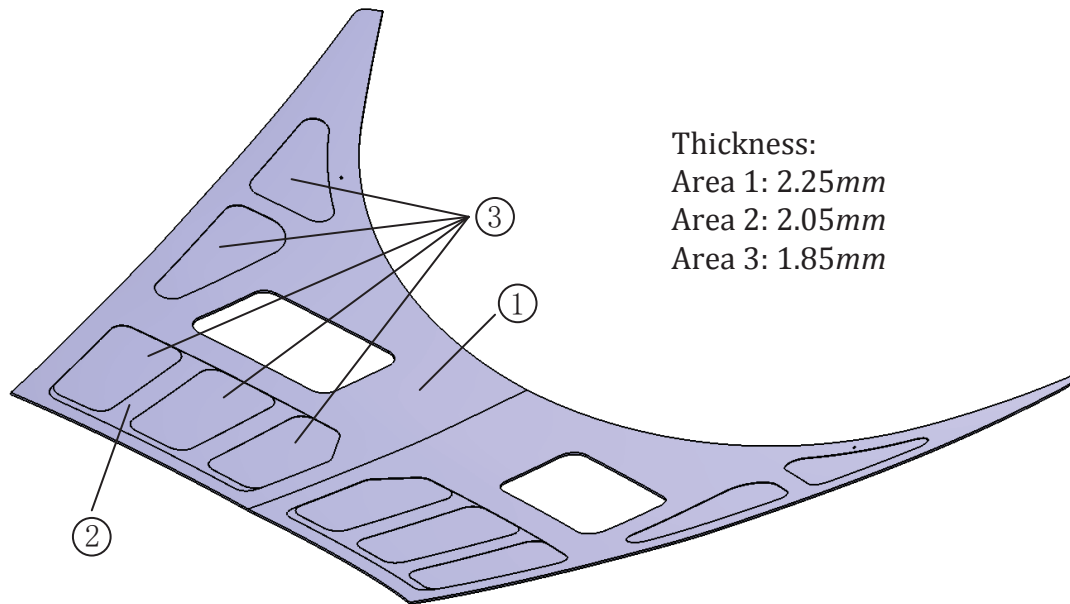
Figure 4.1   Designed part of example 1

Table 4.1 shows the maximum springback value in Z direction in five iterations.

Although it varies a little bit, by undergoing the same stretch forming process, they could

all reach the level around 5mm.
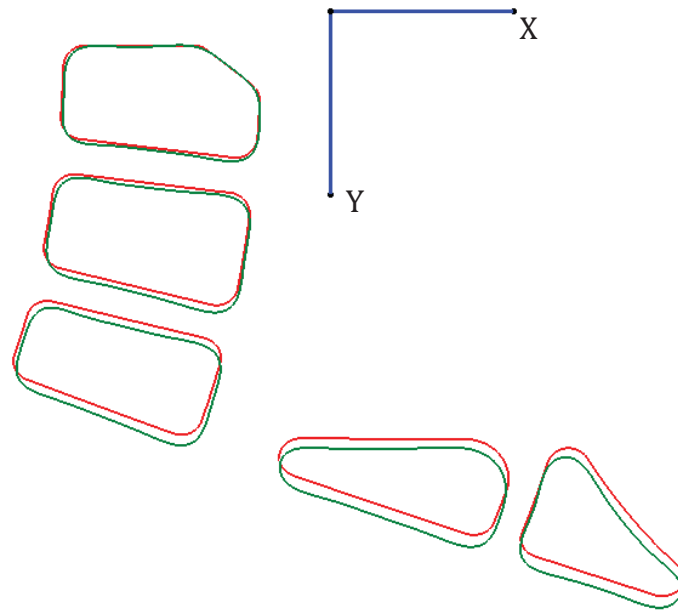
Figure 4.2   Shape deviation comparison in XY plane between the target profile and

deformed profile of first iteration

Table 4.1   Maximum springback value in five iterations of example 1

Iterations No.	Max. springback value in Z direction (*mm*)
1	5.413
2	5.334
3	5.471
4	5.18
5	5.226

For the deviation in X and Y directions, Figure 4.3 shows the numbering of the profiles and partial view of the deformed profiles of each iteration. Table 4.2 gives a detail of the maximum deviation on XY plane.
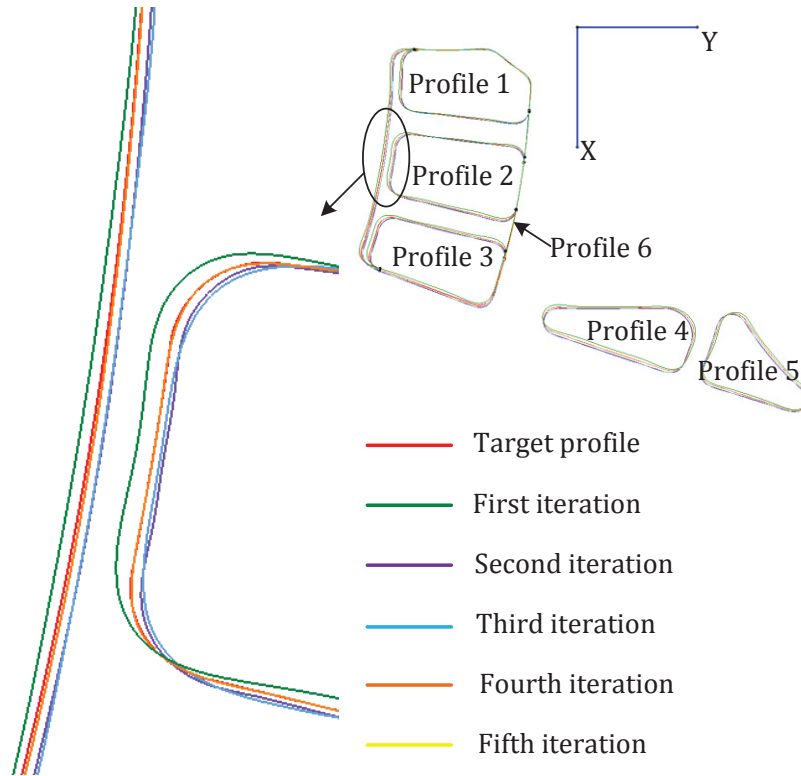
Figure 4.3   Evaluation of the shape deviation in X and Y directions of example 1

Table 4.2   Maximum deviations between the formed profiles and the target profiles on XY plane of example 1

Max. deviation (*mm*)	Profile 1	Profile 2	Profile 3	Profile 4	Profile 5	Profile 6
Iteration 1	2.137	3.647	4.066	3.575	3.082	3.158
Iteration 2	1.51	2.676	2.456	3.072	2.443	2.066
Iteration 3	0.75	1.212	1.095	1.543	1.041	1.272
Iteration 4	0.472	0.427	0.672	0.371	0.421	0.761
Iteration 5	0.47	0.375	0.663	0.556	0.3	0.729

The thickness distribution of area 1, area 2, and area 3 are shown in Figure 4.4, Figure 4.5, Figure 4.6 respectively.
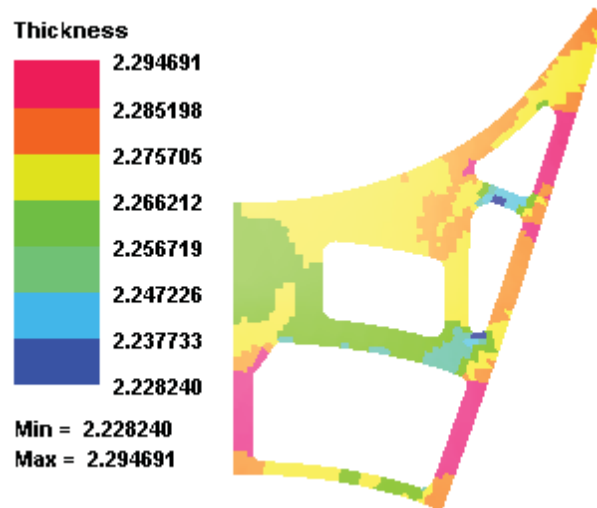
Figure 4.4   Thickness distribution of area 1 of example 1
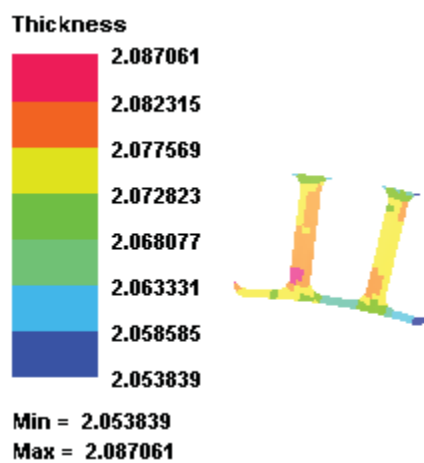
Figure 4.5   Thickness distribution of area 2 of example 1
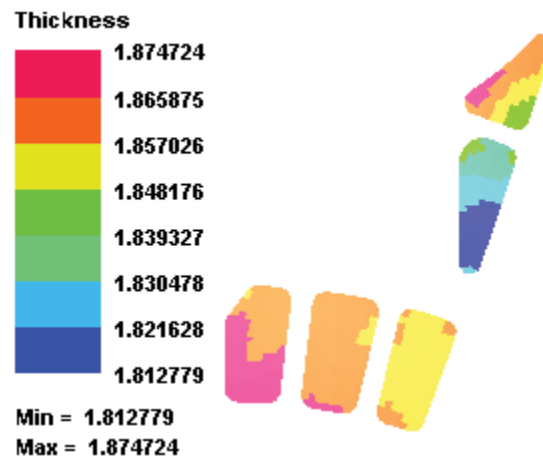
Figure 4.6   Thickness distribution of area 3 of example 1

From this example, it could be found that, even for an additional pocket area designed with different thickness, the method for method for flat blank design is still feasible and reliable.

4.2 Example 2

The real aircraft skins stretching formed are usually designed with large dimensions. To verify the feasibility and reliability of the blank design method with large dimension and more pockets features, a large size of the aircraft skin is proposed as Figure 4.7. The target thickness of the part also could be found.

307*mm*

1282*mm*

1944*mm*

Target thickness:
Pocket area: 1.85*mm*
Panel: 2.45*mm*
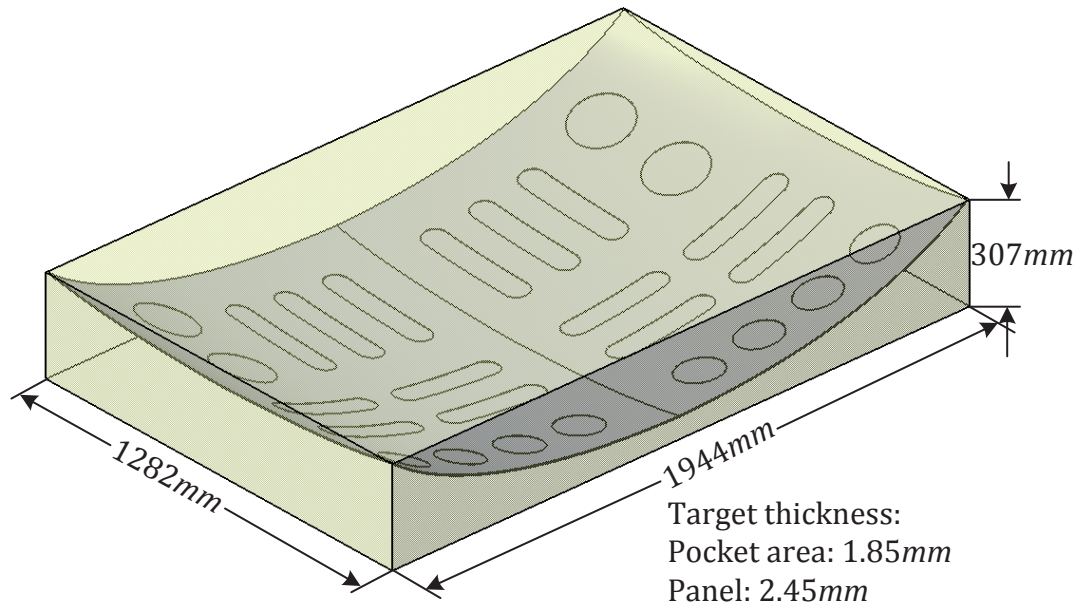
Figure 4.7   Designed part of example 2

First for the initial blank assumption, the pockets positions are determined by unfolding function. To determine the outline of the blank, due to the large size of the part, additional length need to be added to effectively minimize the springback value, so the blank size is selected as 2830$mm \times$1550mm. By conducting the FEA simulation and employing the optimization method, the springback value is minimized around 8mm, as Table 4.3 shows, which is relatively large compared with the previous example because of the size of the designed part. For the deviations in XY plane, by applying the sensitivity method, it showed a good result as Table 4.4, and after four iterations, the maximum deviation could reach to the level of 0.5mm to 0.7mm, which stays in the same level of the previous examples. In the following fifth iteration, it did not show the

improvement of the deviation. The thickness distribution for the pockets area is in the

range of 1.8213mm~1.8878mm and the pockets area is around $2.403mm$~$2.481mm$.

Table 4.3   Maximum springback value in five iterations of example 2

Iterations No.	Max. springback value in Z direction (mm)
1	8.249
2	8.106
3	9.085
4	8.738
5	8.059

Table 4.4   Maximum deviations between the formed profiles and the target profiles on XY plane of example 2

Max. deviation (mm)	Iteration 1	Iteration 2	Iteration 3	Iteration 4	Iteration 5
Profile 1	5.872	2.982	0.914	0.693	0.691
Profile 2	6.687	3.911	1.215	0.55	0.79
Profile 3	8.217	3.225	1.189	0.663	0.79
Profile 4	11.755	4.173	1.527	0.777	0.91
Profile 5	7.398	3.033	1.179	0.525	0.573
Profile 6	12.648	4.904	1.514	0.691	0.533
Profile 7	7.305	2.852	1.005	0.655	0.52
Profile 8	12.471	3.37	1.94	0.703	0.526
Profile 9	10.156	2.542	0.917	0.286	0.531
Profile 10	10.587	3.003	1.523	0.569	0.518
Profile 11	5.683	2.268	0.716	0.447	0.44
Profile 12	11.98	4.983	1.236	0.619	0.773
Profile 13	12.113	3.161	1.074	0.585	0.708

From the example 2, it also proved that for the aircraft skin with large dimensions

and multi features, the method for flat blank design is still feasible and reliable.

CHAPTER 5   Conclusions and Future Work

5.1 Conclusions

In this work, a new approach is proposed for the manufacture of the aircraft skin by machining the pockets on the flat blank and then performing the stretching.   To ensure the accuracy of simulation, the kinematic movement of the stretching machine, the properties of the materials are analyzed. For the simulation result of the deformed part, the position and shape are checked in X, Y and Z three directions respectively. Comparing to the traditional method of aircraft skin manufacture that machining the pocket features on the stretched panel, it solved the issue of machining accuracy on the curved surface, whose curvature is slightly varied from the designed part due to the springback phenomenon. The major improvements and contributions of this thesis can be summed up in the following aspects:

To check the deviation between the deformed part and the designed part in Z direction, the optimization method is employed to obtain the optimal stretching process parameters by minimization of the maximum springback value. Each stretching stage is analyzed and the possible movements are designed based on the stretching machine.

To evaluate the deviation in X and Y directions and find the mapping relationship of the pockets on the flat blank, initial flat blank is assumed by unfolding the designed part on XY plane and then performing the FEA simulation. Based on the deviation between the deformed part and the designed part in X and Y directions, the blank design is updated by applying the shape sensitivity method. Then conduct the second iteration of simulation until the deviation has reached the requirement.

The results of the applications prove the feasibility and reliability of this method. By employing the sensitivity method, the deviation always could converge to the level around $0.3mm$ to $0.6mm$. The quality evaluation by FLD curve shows a qualified part. Also, due to the limitation of the FEA method, the possible reason for the final level of deviation is mentioned.

5.2 Future work

For future research, the following topics can be considered to expand the present work:

To obtain the accuracy simulation of the stretching forming process, the process parameters of friction coefficient, temperature are changing during the stretching process and they have some effects on the formed part, they could be taken into

consideration if those data are known.

The feature of the slot of the slot could be considered. Due to the stress concentration, a solution could be proposed that the slots are machined before the stretching process and without quality defects.

An automatic system could be developed. According to the input of a designed panel, a system comprising CAD model analysis, FEA simulation, optimization calculation and flat blank design modification could output the optimal blank.

Bibliography

1. Parris, A. N. (1996). *Precision stretch forming of metal for precision assembly* (Doctoral dissertation, Massachusetts Institute of Technology).

2. Wisselink, H. H., & van den Boogaard, A. H. (2005, August). Finite element simulation of the stretch-forming of aircraft skins. In *AIP Conference Proceedings* (Vol. 778, No. A, p. 60). IOP INSTITUTE OF PHYSICS PUBLISHING LTD.

3. Zhang, Y., Zhou, X., Luo, H., & Li, X. (2006). Optimization and validation of loading trajectory for double curve aircraft skin stretch forming process. *Zhongguo Jixie GongchengChina Mechanical Engineering, 17*(19), 2053-2056.

4. Zhang, Y. M., & Zhou, X. B. (2006). Parameter Optimization in Aircraft Skin Stretch Forming Process. *ACTA AERONAUTICA ET ASTRONAUTICA SINICA-SERIES A AND B-, 27*(6), 1203.

5. Han, J. Q., Wan, M., & Chen, X. M. (2009). Optimization of process parameters in stretch forming of aircraft complex skin. *Journal of Plasticity Engineering*, 6, 019.

6. He, D. H., Li, D. S. & Li, L. Q. (2009). Design and optimization of the loading trajectory in aircraft skin drape forming process. *Journal of Plasticity Engineering*, 6, 020.

7. Liu, Y. C. & Zhou, X. B. (2004). Mechanism motion analysis of the skin stretch-forming machine. *Aeronautical Manufacturing Technology*, 1, 85-88.

8. HE, D. H., LI, D. S., TUN, Z. M., & LI, X. J. (2010)Design of Displacement Loading for Aircraft Skin in NC Stretch Forming. *China Mechanical Engineering*, 2, 137-140.

9. Karima, M. (1989). Blank development and tooling design for drawn parts using a modified slip line field based approach. *Journal of Engineering for Industry, 111* (4), 345-350.

10. Vogel, J. H., & Lee, D. (1990). An analysis method for deep drawing process design. *International Journal of Mechanical Sciences, 32*(11), 891-907.

11. Chen, X., & Sowerby, R. (1992). The development of ideal blank shapes by the method of plane stress characteristics. *International journal of mechanical sciences, 34*(2), 159-166.

12. Chen, X., & Sowerby, R. (1996). Blank development and the prediction of earing

in cup drawing. *International journal of mechanical sciences, 38*(5), 509-516.

13. Kuwabara, T., & Si, W. H. (1997). PC-based blank design system for deep-drawing irregularly shaped prismatic shells with arbitrarily shape flange. *Journal of materials processing technology, 63*(1), 89-94.

14. Parsa, M. H., Matin, P. H., & Mashhadi, M. M. (2004). Improvement of initial blank shape for intricate products using slip line field. *Journal of materials processing technology, 145*(1), 21-26.

15. Sowerby, R., Duncan, J. L., & Chu, E. (1986). The modelling of sheet metal stampings. *International journal of mechanical sciences, 28*(7), 415-430.

16. Blount, G. N., & Fischer, B. V. (1995). Computerised blank shape prediction for sheet metal components having doubly-curved surfaces. *THE INTERNATIONAL JOURNAL OF PRODUCTION RESEARCH, 33*(4), 993-1005.

17. Gerdeen, J. C., & Chen, P. (1989, June). Geometric mapping method of computer modeling of sheet metal forming. In *Numiform* (Vol. 89, pp. 437-444).

18. Barlet, O., Batoz, J. L., Guo, Y. Q., Mercier, F., Naceur, H., & Knopf-Lenoir, C. (1996). Optimum design of blank contours using the inverse approach and a mathematical programming technique. In *Numisheet* (Vol. 96, pp. 178-185).

19. Guo, Y. Q., Batoz, J. L., Naceur, H., Bouabdallah, S., Mercier, F., & Barlet, O. (2000). Recent developments on the analysis and optimum design of sheet metal forming parts using a simplified inverse approach. *Computers & Structures*, *78*(1), 133-148.

20. Guo, Y. Q., Naceur, H., Debray, K., & Bogard, F. (2003). Initial solution estimation to speed up inverse approach in stamping modeling. *Engineering Computations* , *20*(7), 810-834.

21. Tang, B. T., Zhao, Z., Lu, X. Y., Wang, Z. Q., Zhao, X. W., & Chen, S. Y. (2007). Fast thickness prediction and blank design in sheet metal forming based on an enhanced inverse analysis method. *International journal of mechanical sciences*, *49*(9), 1018-1028.

22. Parsa, M. H., & Pournia, P. (2007). Optimization of initial blank shape predicted based on inverse finite element method. *Finite elements in analysis and design*, *43*(3), 218-233.

23. Toh, C. H., & Kobayashi, S. (1985). Deformation analysis and blank design in square cup drawing. *International Journal of Machine Tool Design and Research*,

25(1), 15-32.

24. Kim, N., & Kobayashi, S. (1986). Blank design in rectangular cup drawing by an approximate method, *International Journal of Machine Tool Design and Research*, *26*(2), 125-135.

25. Guo, Y. Q., Batoz, J. L., Detraux, J. M., & Duroux, P. (1990). Finite element procedures for strain estimations of sheet metal forming parts. *International Journal for Numerical Methods in Engineering*, *30*(8), 1385-1401.

26. Barlat, F., Chung, K., & Richmond, O. (1994). Anisotropic plastic potentials for polycrystals and application to the design of optimum blank shapes in sheet forming. *Metallurgical and Materials Transactions A*, *25*(6), 1209-1216.

27. Park, S. H., Yoon, J. W., Yang, D. Y., & Kim, Y. H. (1999). Optimum blank design in sheet metal forming by the deformation path iteration method. *International Journal of Mechanical Sciences*, *41*(10), 1217-1232.

28. Shim, H. B., & Son, K. C. (2001). Optimal blank design for the drawings of arbitrary shapes by the sensitivity method. *Journal of engineering materials and technology*, *123*(4), 468-475.

29. Biglari, F. R., Agahi, A., Nikfarjam, O., & Nikbin, K. (2006). Optimum Blank Design Based on Modified Sensitivity Approach. *stress*, *31*, 208.

30. Jin, C. H., Zhou, X. B., Diao, K. S., & Li, X. X. (2004). Springback analysis for stretch bending of aluminum profile. *Cailiao Kexue Yu Gongyi(Material Science and Technology)(China)*, *12*(4), 394-397.

31. Diao, K. S., Zhou, X. B., Li, X. X. (2005). Stretch bending of aluminum extrusion. *Journal of Beijing University of Aeronautics and Astronautics, 31*(2), 134-137.

32. Jin, Z. H., Zhou, X. B. & Diao, K. S. (2004) Numerical simulation of stretch-bending process for extruded aluminum rectangular tubes. *Materials Science & Technology, 12*(6), 572-575.

33. Clausen, A. H., Hopperstad, O. S., & Langseth, M. (2000). Stretch bending of aluminium extrusions for car bumpers. *Journal of Materials Processing Technology*, *102*(1), 241-248.

34. Tongxi, X. Y., & Zhang, L. (1996). Plastic bending: theory and applications (Vol. 2). World Scientific.

35. Lin, S. B., & Ding, J. L. (1995). Experimental study of the plastic yielding of rolled

sheet metals with the cruciform plate specimen. International journal of plasticity, 11(5), 583-604.

36. Barlat, F., Maeda, Y., Chung, K., Yanagawa, M., Brem, J. C., Hayashida, Y., ... & Makosey, S. (1997). Yield function development for aluminum alloy sheets. Journal of the Mechanics and Physics of Solids, 45(11), 1727-1763.

37. Taguchi, G., Jugulum, R., & Taguchi, S. (2004). *Computer-based robust engineering: essentials for DFSS*. ASQ Quality Press.

38. Bolboacă, S. D., & Jäntschi, L. (2007). Design of experiments: Useful orthogonal arrays for number of experiments from 4 to 16. *Entropy*, *9*(4), 198-232.